

MoO₃@Activated Carbon derived from Wheat Straw as a Bi-Functional Electrocatalyst for Efficient Water Splitting



By

Muhammad Usman Khan

Reg. No.: 00000326911

Session 2020-22

Supervised by

Dr. Muhammad Hassan

U.S.-Pakistan Center for Advanced Studies in Energy (USPCAS-E)

National University of Sciences and Technology (NUST)

H-12, Islamabad 44000, Pakistan

November 2023

MoO₃@ Activated Carbon derived from Wheat Straw as a Bi-Functional Electrocatalyst for Efficient Water Splitting



By

Muhammad Usman Khan

Reg. No.: 00000326911

Session 2020-22

Supervised by

Dr. Muhammad Hassan

**A Thesis Submitted to U.S.-Pakistan Center for Advanced Studies in
Energy in partial fulfillment of the requirement for the degree of**

**MASTERS of SCIENCE in
ENERGY SYSTEMS ENGINEERING**

U.S.-Pakistan Center for Advanced Studies in Energy (USPCAS-E)

National University of Sciences and Technology (NUST)

H-12, Islamabad 44000, Pakistan

November 20

THESIS ACCEPTANCE CERTIFICATE

Certified that final copy of MS/MPhil thesis written by Mr. Muhammad Usman Khan (Registration No. 00000326911), of U.S.-Pakistan Center for Advanced Studies in Energy has been vetted by undersigned, found complete in all respects as per NUST Statues/Regulations, is within similarity indices limit and accepted as partial fulfillment for award of MS/MPhil degree. It is further certified that necessary amendments as pointed out by GEC members of the scholar have also been incorporated in the said thesis.

Signature:

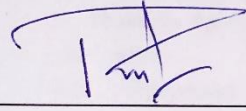


Name of Supervisor: Dr. Muhammad Hassan

Date:

19-12-2023

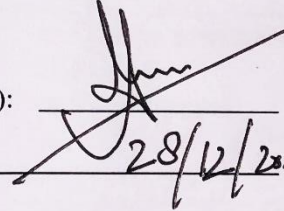
Signature (HoD):



Date:

21-12-2023

Signature (Dean/Principle):



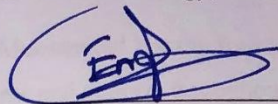
Date:

28/12/2023

Certificate

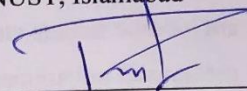
This is to certify that the work in this thesis has been carried out by **Mr. Muhammad Usman Khan** and completed under my supervision in Biofuel Lab, U.S.-Pakistan Center for Advanced Studies in Energy (USPCAS-E), National University of Sciences and Technology, H-12, Islamabad, Pakistan.

Supervisor:



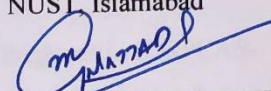
Dr. Muhammad Hassan
USPCAS-E
NUST, Islamabad

GEC member # 1



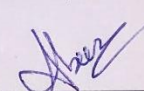
Dr. Rabia Liaquat
USPCAS-E
NUST, Islamabad

GEC member # 2:



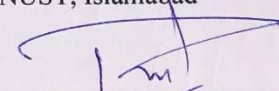
Dr. Mustafa Anwar
USPCAS-E
NUST, Islamabad

GEC member # 3:



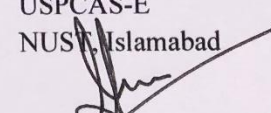
Dr. Abeera Ayaz Ansari
USPCAS-E
NUST, Islamabad

HoD-ESE:



Dr. Rabia Liaquat
USPCAS-E
NUST, Islamabad

Dean/Principal:



Prof. Dr. Adeel Waqas
USPCAS-E
NUST, Islamabad

Acknowledgements

First and foremost, all praise belong to Allah Almighty, the Most Benevolent, the Most Merciful, who has granted me the strength, persistence, courage, and willpower to pursue this work and bring it towards completion.

I would like to express my sincere gratitude to my supervisor, Dr. Muhammad Hassan for his brilliant supervision, a continued source of guidance, encouragements and support throughout my master's research and thesis phase. I have been fortunate to find supervisors who cared deeply about my research progress and answered my every query in timely manner. It would not have been possible to conduct this research or finish my postgraduate studies without his invaluable mentorship. I would also like to thank my Guidance and Examination Committee (GEC) members, Dr. Mustafa Anwar, Dr. Rabia Liaquat, and Dr. Abeera Ayaz Ansari for their advice and support through various stages of the project.

Finally, I would also like to thank the Department of Energy Systems Engineering, USPCAS-E, NUST, my parents, brothers, my colleagues, and peers for their continuous support during my MS journey.

Dedication

In the profound tapestry of this thesis, I offer my deepest gratitude to my late grandmother, "Ami," the eternal presence whose wisdom and love continue to illuminate my path. Her legacy of resilience and kindness infuses every word written here, reminding me of the strength found in gentleness. To my cherished parents, the guiding stars in my life's constellation, who bestowed upon me the profound lessons of resilience and perseverance, shaping me into the person I am today. My father, a pillar of unwavering support through life's tempests, my mother, the embodiment of patience and relentless determination, and my older brother, a beacon of courage, have been my unyielding rocks. Alongside, my younger brother, a wellspring of boundless inspiration, has shown me the beauty of unwavering spirit. To my teachers, whose wisdom and mentorship have been my compass, and my friends, whose shared laughter and shared tears have enriched every chapter of this journey, I owe a debt of gratitude. This work is not just a culmination of academic endeavor; it echoes with the collective wisdom, love, and resilience of each of these remarkable individuals. Their influence is not only reflected in these pages but also in the very essence of my being. With profound appreciation, I recognize the profound impact of their presence, shaping not just this thesis but the life it represents.

Abstract

Hydrogen is often seen as an attractive alternative to traditional fossil fuel sources since it is seen as a highly promising and environmentally sustainable energy carrier. Water splitting is a low-cost method for producing hydrogen that can be accomplished through the use of light or electricity. An effective catalyst is required to lower the considerable overpotential value produced by the Hydrogen Evolution Reaction (HER) and the Oxygen Evolution Reaction (OER) during water splitting. In this study, Wheat Straw-based activated carbon (AC) and MoO₃ loaded on AC, referred to as MoO₃@AC, were employed as electrocatalysts on nickel foam for the purpose of water splitting. The synthesis of the electrocatalyst MoO₃@AC involved the utilization of a 1:1 ratio of AC to MoO₃. The resulting electrocatalyst, MoO₃@AC, demonstrated remarkable performance in terms of overpotential for the HER, measuring at 86.4 mV, and for the OER, measuring at 146.6 mV. Additionally, the electrocatalyst exhibited favourable tafel slopes of 90 mV/dec and 104 mV/dec for the HER and OER, respectively.

Keywords: *Water splitting; HER; OER; Hydrogen Production; Activated Carbon (AC)*

Table of Contents

Abstract.....	vii
Table of Contents.....	viii
List of Figures.....	x
List of Tables.....	xi
List of Publications.....	xii
Abbreviations.....	xiii
Chapter 1.....	1
Introduction.....	1
1.1. Overview of Research.....	1
1.2. Problem Statement.....	4
1.3. Research Problem and Hypothesis.....	5
1.4. Objectives.....	5
1.5. Scope of Work.....	5
1.6. Outline.....	6
Summary.....	6
Chapter 2.....	8
Literature Review.....	8
2.1. Overview.....	8
2.2. Hydrogen Production.....	9
2.2.1. Electrochemical Water-Splitting.....	11
2.3. Common Materials in Electrochemical Water-Splitting.....	14
2.3.1. Fe-based Metal Organic Framework (MOF).....	14
2.3.2. Transition Metal Carbides/Nitrides.....	15
2.3.3. Transition Metal Selenides.....	15
2.3.4. Activated Carbon based Materials.....	15
2.3.5. Transition Metal Oxides.....	16

Summary	16
Chapter 3	17
Materials and Methods	17
3.1. Synthesis	17
3.1.1. Materials	17
3.1.2. Making of Wheat Straw Activated Carbon WSAC	18
3.1.3. Synthesis of MoO ₃ Loaded Activated Carbon (MoO ₃ @AC)	18
3.2. Catalyst Characterization and Techniques Overview	19
3.2.1. X-Ray Diffraction (XRD)	19
3.2.2. Scanning Electron Microscopy (SEM)	20
3.2.3. Raman Spectroscopy	21
3.2.4. N ₂ Adsorption – Desorption	23
3.3. Experimental Setup for Electrochemical Measurements	23
Summary	25
Chapter 4	26
Results and Discussion	26
4.1. Physicochemical Properties of the Electrocatalyst	26
4.2. Electrocatalysts Electrochemical Performance	30
Summary	34
Chapter 5	35
Conclusions and Recommendations	35
5.1. Conclusions	35
5.2. Recommendations	36
References	37

List of Figures

Figure 1.1: Thesis Flowchart	6
Figure 2.1: Techniques of Hydrogen production.....	10
Figure 2.2: Color-coded representation of the three distinct pathways for producing hydrogen (H ₂).....	11
Figure 2.3: HER Proposed Mechanism	13
Figure 3.1: Schematic Diagram for electrocatalyst synthesis.....	19
Figure 3.2: Energy level diagram in Raman spectroscopy	22
Figure 3.3: Electrochemical workstation setup.....	24
Figure 3.4: Three Electrodes System	24
Figure 4.1: XRD of AC and MoO ₃ @AC.....	26
Figure 4.2: SEM images of (A) AC at 50 μm and (B) MoO ₃ @AC at 50 μm	27
Figure 4.3: EDS of (A) AC and (B) MoO ₃ @AC.....	27
Figure 4.4: Raman Spectra of AC and MoO ₃ @AC	28
Figure 4.5: N ₂ Adsorption-Desorption Isotherm	29
Figure 4.6: (A) HER (LSV Curves), (B) MoO ₃ @AC, AC and NF Overpotentials, (C) Tafel plots for HER	30
Figure 4.7: (A) OER (LSV curves), (B) MoO ₃ @AC, AC and NF (Overpotentials), (C) Tafel plots for OER	32
Figure 4.8: (A) CV for AC, (B) CV for MoO ₃ @AC, (C) EIS for AC and MoO ₃ @AC.....	34

List of Tables

Table 4.1: Summary of N ₂ Adsorption-Desorption	29
Table 4.2: Resistances for AC and MoO ₃ @AC obtained from EIS.	33
Table 4.3: Comparison of recent studies conducted on AC and MoO ₃ with the synthesized electrocatalysts.....	34

List of Publications

- 1- **MoO₃@Activated Carbon derived from Wheat Straw as a Bi-Functional Electrocatalyst for Efficient Water Splitting (Under submission)**

Abbreviations

AC	Activated Carbon
BET	Brunauer – Emmett – Teller surface area analysis
BJH	Barrett, Joyner, and Halenda method
CV	Cyclic voltammetry
EDS	Energy-dispersive X-ray spectroscopy
EIS	Impedance spectroscopy
GHGs	Greenhouse gases
HER	HER
LSV	Linear sweep voltammetry
OER	OER
RHE	Reversible hydrogen electrode
WSC	Wheat Straw Char

Chapter 1

Introduction

1.1. Overview of Research

The escalating demand for energy in contemporary society underscores its indispensability as a vital commodity. The increasing demand for energy is a direct consequence of technological advancements. Fossil fuels have served as a substantial and noteworthy energy storage medium for approximately the past 150 years. Coal, oil, and natural gas are highly concentrated sources of energy that can be conveniently stored in solid, liquid, or gaseous forms. The ability to access the energy stored in fossil fuels aligns with the demand-side requirements of the energy system. The increase in electricity demand prompts the power plant to augment its fuel input, thereby facilitating a corresponding escalation in electricity generation. The significance of this phenomenon lies in the fact that the availability of on-demand energy, facilitated by the utilization of fossil fuels, has resulted in a highly rigid energy system. This rigidity stems from the expectations of energy consumers, who anticipate immediate access to energy whenever it is required.

The present discourse acknowledges that several factors in contemporary times contribute to the suboptimal nature of fossil fuels. The rapid depletion of fossil fuels is evident, despite their previous abundance [1]. The heavy reliance on fossil fuels for energy generation in contemporary technology poses a significant problem. The majority of engines and turbines worldwide rely on the combustion of various fossil fuels. The scientific community has long been cautioning about the detrimental effects of excessive fossil fuel consumption and the subsequent release of harmful pollutants. Undoubtedly, the escalating prevalence of Global Warming and Climate Change has emerged as a significant concern in contemporary society.

The combustion of fossil fuels constitutes the primary source of anthropogenic carbon dioxide (CO₂) emissions into the Earth's atmosphere. The absorption of approximately 2.0 ± 0.8 Gt/year of CO₂ by the ocean has been identified as a significant factor contributing to the process of acidification, which subsequently poses detrimental effects on coral reefs and various ecological systems. The current imbalance in atmospheric CO₂ concentration, which has not been observed for over a million years, can be attributed to a combination of factors

including the emission of CO₂ during cement manufacturing, deforestation, and soil disturbance. The Earth's system has experienced an augmentation in energy retention, leading to a notable elevation of 0.8 °C in the global average temperature. The observed alteration in average conditions has resulted in a notable augmentation in both the frequency and magnitude of extreme weather phenomena, including but not limited to severe storms, floods, droughts, and heat waves. This study examines the potential consequences of introducing an additional 565 gigatons of CO₂ into the atmosphere and its implications for the likelihood of triggering catastrophic climate change. The findings suggest that there is a minimum probability of one in five for such an event to occur. In order to mitigate the risk of an uncontrollable climate change, it is imperative to curtail fossil fuel combustion by 90% before the year 2050. The present analysis highlights the latest assessments pertaining to the quantifiable reserves of fossil fuels that can be viably extracted for economic purposes. These estimations project a cumulative emission of approximately 2795 gigatons of carbon dioxide (Gt CO₂). The world's current trajectory implies an inevitable climate catastrophe [2].

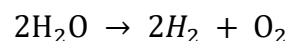
The pursuit of alternative fuel as a replacement for conventional fossil fuels has become a paramount concern for researchers and innovators worldwide, prompted by the aforementioned issues. The community's commitment to change is evident in the advocacy for Electric Vehicles, Solar Power Plants, Wind Turbine farms, and similar initiatives.

The notion of a hydrogen economy was initially introduced by Jules Verne, a visionary author, in the 1870s through his speculative work, *The Mysterious Island* [3]. The concept of the "hydrogen economy" emerged in 1970 when John Bockris introduced the term during a presentation at General Motors. The central premise of the hydrogen economy revolves around the production of hydrogen utilizing preexisting energy sources. In the near future, hydrogen has the potential to supplant the prevailing utilization of fossil fuels in various sectors, including industries, residences, and transportation. The concept of the hydrogen economy presents itself as a potential solution to a range of urgent and interconnected global challenges. These challenges include but are not limited to: (i) the pressing environmental issues that have a worldwide impact, (ii) the depletion of natural resources, (iii) the scarcity of food in developing nations, and (iv) the continuous growth of the global population [4].

In the 1970s, extensive research on hydrogen production was conducted by experts from the Institute of Nuclear Energy in Vienna and the Electric Power Research Institute. The primary objective of this study is to explore the production of hydrogen gas through nuclear

reactions, with the subsequent utilization of this hydrogen gas for electricity generation. The ultimate replacement of fossil fuels is envisioned. The study's findings demonstrate that the utilization of high temperature thermonuclear methods for hydrogen production surpasses the efficiency and cost-effectiveness of hydrogen production through electrolysis [5,6]. The study conducted revealed that the direct generation of electricity from nuclear plants exhibited superior cost-effectiveness and efficiency in comparison to the utilization of hydrogen for electricity production through fuel cell technology.

The chemical binding of hydrogen, despite its abundance on Earth, predominantly restricts its availability. In order for a substance to be utilized as a fuel source, it is imperative that it exists in its molecular state or in a state where it is not bound to other elements or compounds. The central issue at hand pertains to the considerable energy demand associated with the acquisition of unbound hydrogen. The feasibility of utilizing hydrogen gas as a fuel is hindered by the significant disparity between the energy expended in its production and the energy generated when it is employed as a source of energy. The equation presented demonstrates that the breakdown of a water molecule into hydrogen and oxygen necessitates an energy input of 120 MJ/kg-hydrogen. The reverse reaction, in an ideal scenario, results in the production of 120 MJ/kg-hydrogen. In the context of real-world scenarios, it is imperative to acknowledge that ideal reactions are not attainable. Consequently, it becomes necessary to input an energy exceeding 120 MJ/kg into the initial reaction, while the subsequent recombination process yields an energy recovery of less than 120 MJ/kg.

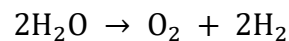
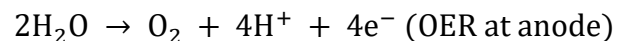


There are several different sources from which the production of hydrogen gas can be derived. These sources include fossil fuels, nuclear materials, and renewable sources. Each of these sources has its own unique characteristics. Firstly, let's consider fossil fuels. These are non-renewable resources that have been formed over millions of years from the remains of ancient plants and animals. Fossil fuels such as coal, oil, and natural gas can be used to produce hydrogen gas. In this study, we explored hydrogen production and some processes that are employed to produce hydrogen i.e., water electrolysis, methane cracking, and several other methods. By thoroughly examining these processes, we aim to shed light on their unique characteristics, advantages, and limitations, providing a comprehensive understanding of hydrogen production. When it comes to the production of hydrogen, there are two separate kinds that can be obtained: "Green Hydrogen" and "Non-Green Hydrogen." These

classifications are determined based on the specific method selected for the production process. There are a few distinct techniques that can be utilized to accomplish the capacity of hydrogen. One choice is to store hydrogen in chambers, where it tends to be kept in its vaporous structure. This strategy takes into consideration simple transportation and openness, as the chambers can be advantageously shipped to various areas depending on the situation. Another methodology is to melt hydrogen, which includes cooling it to low temperatures incredibly. Thusly, hydrogen can be put away in a fluid state, lately, there have been noteworthy turns of events and headways in the field of metal hydride stockpiling, which play had a vital impact in upgrading the practicality and wellbeing of this stockpiling strategy. These improvements have achieved a various positive effects [7].

1.2. Problem Statement

Electrochemical water splitting has acquired huge consideration because of its extraordinary effectiveness and astounding natural advantages. This strategy fills in as a brilliant choice for the production of hydrogen gas, since it brings zero carbon emissions [8]. At the point when we look at the reaction, we can separate it into two separate half reactions. The primary half reaction is known as the Oxygen Evolution Reaction (OER), which happens at the anode. The final reaction is known as the Hydrogen Evolution (HER), and it happens at the cathode. The introduced condition exhibits the reactions [9–11]:



One of the principal challenges that scientists face with regards to creating hydrogen for an enormous scope through the course of water splitting is the requirement for a huge overpotential [12,13]. To really complete the course of electrolysis, the electrolyzer requires a particular standard potential (ΔE) of 1.23 V. This potential is estimated comparative with a reversible hydrogen electrode (RHE). The fundamental target of this electrolysis interaction is to change over water into hydrogen gas (H_2) and oxygen gas (O_2) [14].

In the field of (HER), it is normal to utilize costly metallic catalysts like platinum, iridium, palladium, and rhodium. These catalysts assume an essential part in working with the HER cycle, where hydrogen gas is produced from the splitting of water atoms. Notwithstanding, because of their significant expense, researchers are continually searching

for elective catalysts that can give comparable outcomes at a more reasonable cost [15,16]. These metals present critical challenges as far as commercialization because of their over-the-top costs. Subsequent investigations have substantiated the exceptional efficacy of transition metals, specifically iron, nickel, and cobalt, in various applications. Moreover, their cost-effectiveness renders them readily replaceable in instances where their performance deteriorates under more intense acidic or alkaline circumstances [17–19]. In recent years, a multitude of studies have been conducted, employing diverse compounds comprising multiple elements, with the aim of identifying electrodes that exhibit high efficacy in the process of electrochemical water splitting.

1.3. Research Problem and Hypothesis

In order to meet our forthcoming energy demands, hydrogen (H₂) is regarded as an abundant and environmentally friendly fuel, as evidenced by a range of diverse variations. Participation in the so-called "Hydrogen Economy" appears to have significant importance in contemporary times for governmental bodies, major energy corporations, automobile manufacturers, and related enterprises. The concept is straightforward: harness the abundant element of hydrogen, which is widely available on Earth and throughout the universe, for the purpose of serving as a pristine fuel source or as an energy carrier to power vehicles, provide heating for residential and commercial spaces, generate electricity, and more. The outcome of this process is solely the production of water, without any of the carbon dioxide emissions and other pollutants associated with the consumption of petroleum products, as is the case in the current carbon-based economy.

1.4. Objectives

1. To synthesize and characterize AC and MoO₃ loaded AC i.e., MoO₃@AC electro-catalyst.
2. To analyze the effect of MoO₃ loading on structural and morphological properties of AC.
3. To study the performance of AC and MoO₃@AC as electrocatalysts in water splitting reactions

1.5. Scope of Work

AC and MoO₃@AC were synthesized, and the as synthesized samples were characterized using X-ray diffraction (XRD), field emission scanning electron microscopy (FESEM), energy-dispersive X-ray spectroscopy (EDS), Raman Spectroscopy and N₂

physisorption. Electrochemical measurements were carried out to determine the water splitting potential on an electrochemical workstation. Two and three-electrode assemblies were tested for the materials on the workstation to find out the overall water splitting potential. The working electrodes were made from drop casting the electro-catalyst inks onto nickel foam, Ag/AgCl was used as the reference electrode and Platinum wire was used as the counter electrode.

1.6. Outline

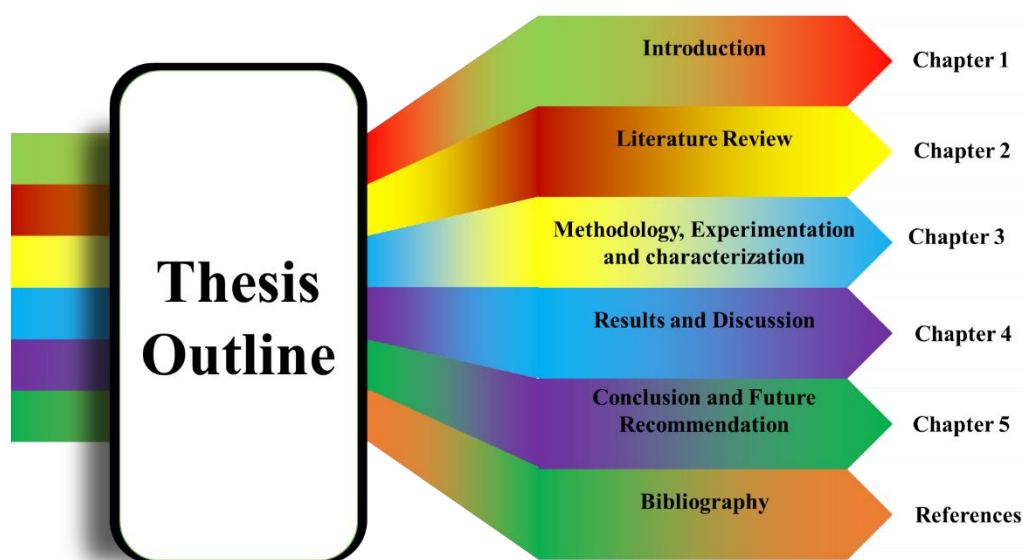


Figure 1.1: Thesis Flowchart

Summary

The contemporary global landscape is characterized by the pressing challenges of energy shortages and climate change. The effective resolution of both aforementioned issues can be achieved through the establishment of commercial viability for green hydrogen. The acquisition of hydrogen gas from various sources is a well-established practice. However, to ensure its ecological sustainability, the preferred method is the utilization of water splitting. The objective of this study is to investigate the development of cost-effective materials for efficient hydrogen (H₂) production from water. Perovskites and double perovskites have emerged as promising materials due to their exceptional tunability and robustness in extreme environments.

This study aims to synthesize MoO₃ loaded activated carbon derived from wheat straw and evaluate its efficacy as an electrocatalyst for water splitting reactions, specifically the HER and OER. Different types of analysis were used to characterize the samples i.e., XRD (X-ray

Diffraction), FESEM (Field Emission Scanning Electron Microscopy), EDS (Energy Dispersive Spectroscopy), Raman Spectroscopy, and BET (Brunauer-Emmett-Teller) analysis.

Chapter 2

Literature Review

2.1. Overview

In the past few decades, there has been a consistent and significant increase in the worldwide need for energy. This surge in demand can be attributed to the continuous processes of industrialization and urbanization that have been developing across the globe. As nations endeavor to create and work on their economies, ventures have thrived, and urban communities have extended at an exceptionally high rate. Subsequently, this quick development has driven a want energy asset to control these developing areas. Industrialization, plays had a critical impact in driving up the worldwide energy interest. As countries look to upgrade their financial result and contend on the worldwide stage, they have progressively depended on modern exercises to build their efficiency. These businesses require critical measures of energy to work their apparatus, power their cycles, and meet the developing necessities of purchasers around the world. These continuous cycles came about a flood in natural debasement. It is vital to take note of that as our general public's interest for energy has developed, so too meaningfully affects the climate [20]. For a long time, individuals have perceived the significance of really utilizing energy to advance practical monetary development and work on personal satisfaction in present day cultures. This acknowledgment comes from the comprehension that energy assumes a crucial part in driving different parts of our lives, from fueling enterprises and transportation frameworks to giving power to homes and organizations [21]. The consumption of petroleum products is a pressing issue that we should address with direness. It is turning out to be progressively certain that ward on them as our essential worldwide energy source is basically not feasible over the long haul. We want to perceive the restricted accessibility of these assets and the effect their extraction and utilization have on our current circumstance. It is significant that we investigate and put resources into elective energy sources that can give us an additional practical and inexhaustible future. Lately, there has been a perceptible expansion in the rate at which we consume energy. This flood in energy utilization has raised worries among numerous people and associations about the effect it has on our current circumstance. We are turning out to be more mindful of the unfortunate results related with our ongoing energy utilization designs, especially the utilization of petroleum derivatives.

Individuals are turning out to be more mindful of the rising measure of energy we use, the effect it has on the climate, and the way that petroleum products are getting more costly. In view of these worries, we are currently investigating different wellsprings of energy that are perfect, sustainable, and can be utilized for quite a while [22–24]. Hydrogen arises as a leader chasing a suitable energy source equipped for fulfilling the worldwide need in a supportable way. Hydrogen gas (H_2) shows an outstandingly raised energy elevation of about 142 megajoules per kilogram (MJ/kg). Also, its combustion process exclusively yields water as a by-product, so rendering it highly environmentally friendly [25]. Hydrogen is widely recognized as a sustainable energy resource that has numerous applications, including but not limited to automotive propulsion, heating systems, and fuel cells. Its utilization is particularly appealing due to its little environmental footprint [26–29]. Hydrogen, being the most prevalent element in the observable universe, is typically found in a state other than its elemental form, with H_2 gas being a very infrequent occurrence. Therefore, it is imperative that an alternative method is employed for the production and subsequent storage of the aforementioned resource, ensuring its efficient utilization whenever required [30].

2.2. Hydrogen Production

The classification of hydrogen production can be broadly categorized into two distinct types based on the raw materials utilized: conventional technologies and renewable technologies. The utilization of conventional techniques in energy production is heavily dependent on fossil fuels, wherein processes such as hydrocarbon reforming and pyrolysis are employed. This study examines the application of chemical techniques, namely steam reforming, partial oxidation, and autothermal steam reforming, in the process of refining hydrocarbon reforming.

The subsequent significant classification covers procedures that are aimed at the production of hydrogen from renewable resources, more especially biomass or water. Both of these are examples of different sources. The classification of methods that make use of biomass as a feedstock for the production of hydrogen is the focus of this investigation, which is presented as a thesis. To be more explicit, the focus is directed on two separate areas, namely biological processes and thermochemical processes. The term "thermochemical processes" refers to a broad category that encompasses many different kinds of reactions, including pyrolysis, gasification, combustion, and liquefaction, amongst others. There are a number of diverse biological processes, including sequential dark and photo-fermentation, dark fermentation, photo-fermentation, and direct and indirect bio-photolysis. The study of

biochemistry requires an understanding of these processes because of their significance, and because they present chances for more research and academic advancement. The purpose of this research is to add to the current body of information and deepen our comprehension of the complex mechanisms at play during bio photolysis, fermentation, and the sequential coupling of these two processes. The accomplishment of this task will be achieved by the examination of the processes that have been previously mentioned. The electrocatalytic splitting of water is an innovative method that aims to achieve the sustained production of hydrogen as a pure and potentially useful source of energy [30]. Hydrogen is produced through the process of splitting water into its individual molecules, this can be achieved through different chemical reactions. Some of these reactions include electrolysis, thermolysis, and photo-electrolysis. Among the raw materials that are utilized in the manufacture of these procedures, water is the one and only one that is utilized [31].

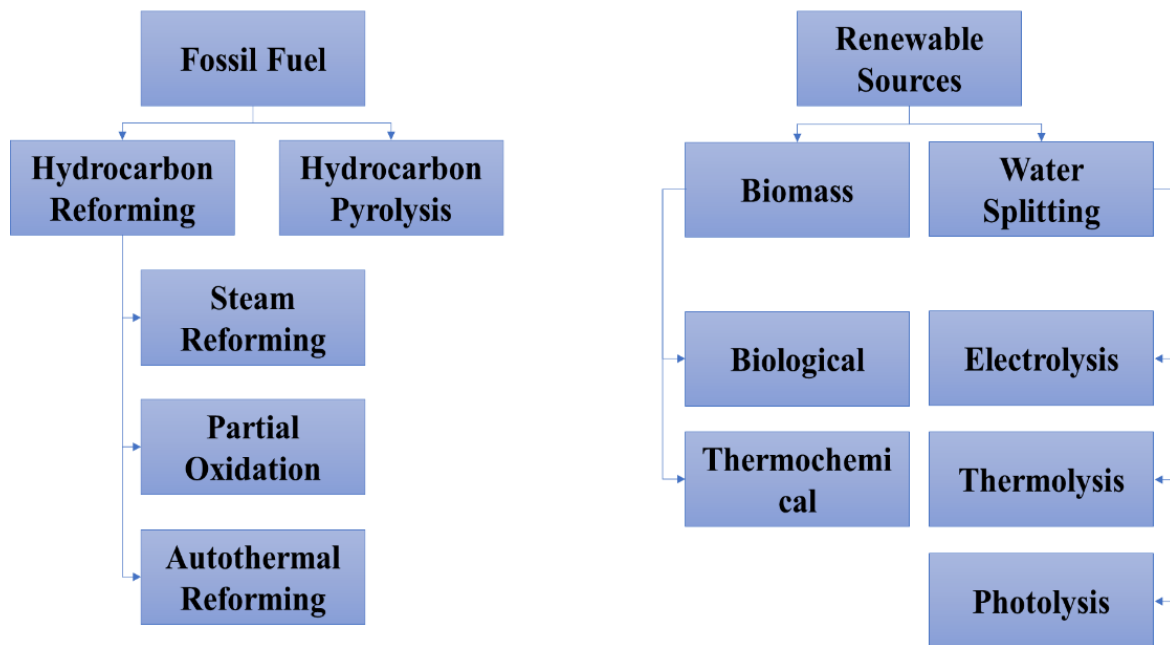


Figure 2.1: Techniques of Hydrogen production[31]

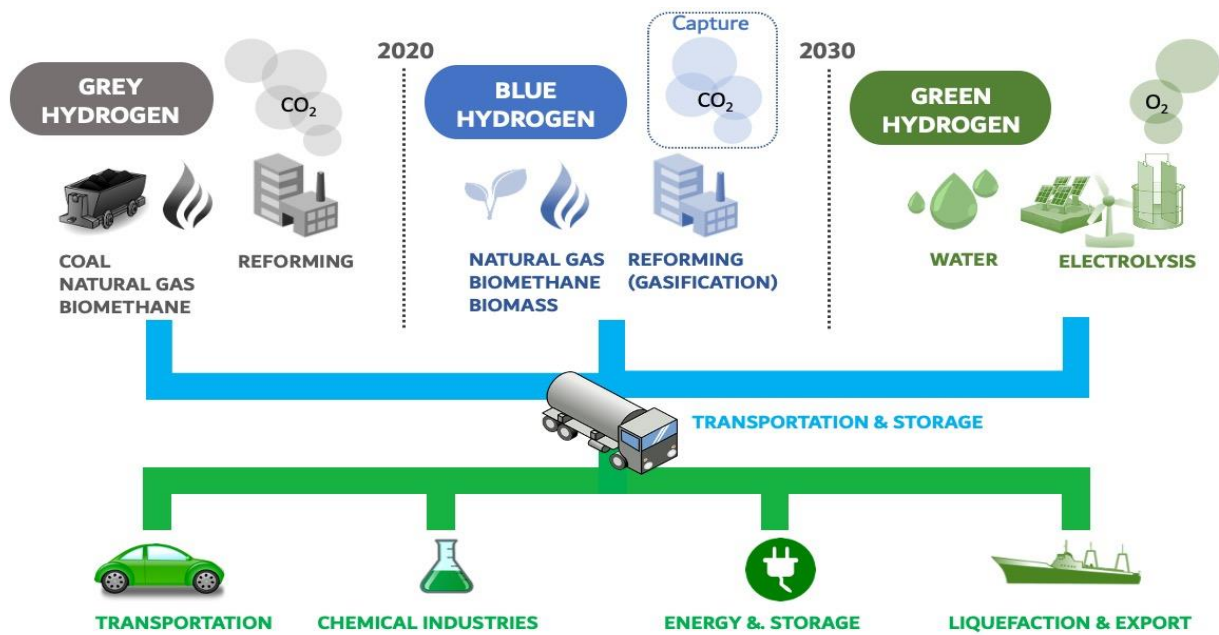
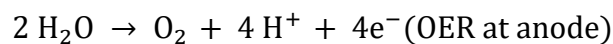
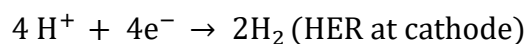


Figure 2.2: Color-coded representation of the three distinct pathways for producing hydrogen (H₂) [32]

2.2.1. Electrochemical Water-Splitting

Electrochemical water splitting is regarded as an ecologically sustainable approach, since it has the potential to generate hydrogen gas and oxygen gas through the electrolysis of water. The theoretical voltage required for this process is commonly accepted to be 1.23 V. When considering practical implementation, it is necessary to apply a voltage of 1.8 V in order to overcome the activation energy barrier of the reaction [33]. The reaction can be divided into two distinct half reactions, namely the OER occurring at the anode and the HER taking place at the cathode. The chemical reactions are depicted in the equation provided below [9–11].



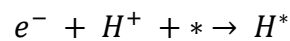
In order to achieve successful water splitting within the electrolyzer, it is theoretically necessary to have a Gibbs free energy (ΔG) of approximately 237.2 kJ/mol and a standard potential (E) of 1.23 V [14]. The main obstacles for large-scale hydrogen generation through water splitting are unfavorable thermodynamics and the requirement of a large overpotential [34,35]. The utilization of costly metals, including platinum, iridium, palladium, and rhodium, as catalysts for the HER has conventionally posed challenges in terms of commercial viability [15,16,36]. Subsequent investigations have substantiated the efficacy of transition metals, specifically iron, nickel, molybdenum and cobalt, in a remarkable manner [17–19,37].

Moreover, their cost-effectiveness renders them readily replaceable in the event of corrosion arising from heightened acidic or alkaline circumstances. In recent years, a plethora of studies have been conducted, employing diverse compounds composed of multiple elements, with the aim of identifying efficacious electrodes for the process of electrochemical water splitting.

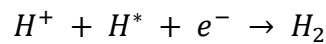
2.2.1.1. Mechanisms for Water-Splitting

Based on evidence from experiments and studies, the following are the essential steps in the HER [35]:

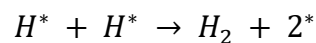
In acidic media:



(The Volmer reaction, electrochemical adsorption, ≈ 120 mV dec⁻¹)

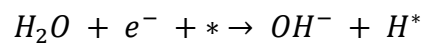


(The Heyrovsky reaction, electrochemical desorption, ≈ 40 mV dec⁻¹)

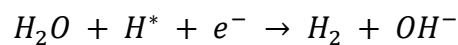


(The Tafel reaction, chemical desorption, ≈ 30 mV dec⁻¹)

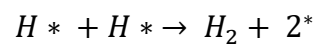
In alkaline or neutral media:



(The Volmer reaction, electrochemical adsorption, ≈ 120 mV dec⁻¹)



(The Heyrovsky reaction, electrochemical desorption, ≈ 40 mV dec⁻¹)



(The Tafel reaction, chemical desorption, ≈ 30 mV dec⁻¹)

In this statement, the active site on the surface of the electrocatalyst is denoted by the symbol *. The Volmer step involves the adsorption of hydrogen atoms onto the surface of the electrocatalysts, facilitated by the favorable conditions provided by the surface. During the Tafel reaction, it is observed that a hydrogen atom (H*) can undergo combination with another hydrogen atom (H*) resulting in the release of a dihydrogen molecule (H₂) as well as the

generation of two active sites. The Heyrovsky reaction involves the potential for the reactant to undergo reactions with H^+ or H_2O in both acidic and alkaline environments [38].

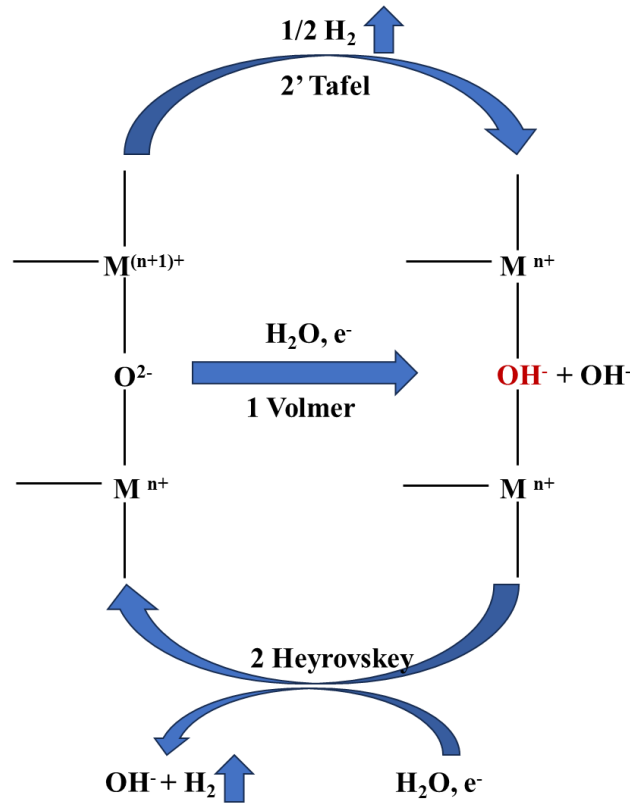
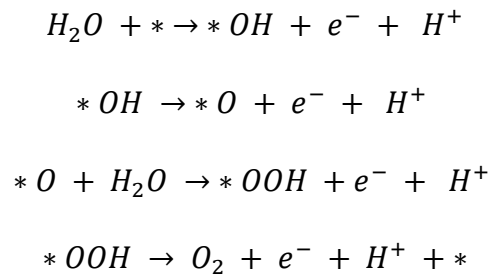


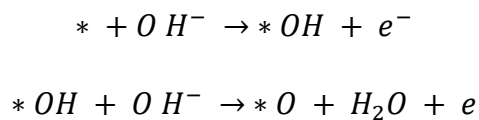
Figure 2.3: HER Proposed Mechanism

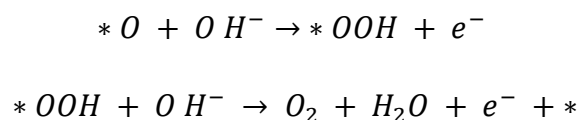
Based on experimental and research data, the OER fundamental phases include the following:

In acidic media:



In alkaline or neutral media:





In this study, the active sites on the surface of the electrocatalysts are denoted by the symbol *. In alkaline media, the hydroxyl radical forms a binding interaction with the active site of the electrocatalyst, resulting in the formation of *OH. The process of electron removal from *OH, coupled with proton transfer, results in the formation of *O. The formation of intermediate OOH* occurs subsequent to the nucleophilic attack of an OH ion onto O*. In conclusion, the occurrence of a proton-coupled electron transfer results in the production of a single oxygen molecule, accompanied by the formation of a free active site.

2.2.1.2. *Criteria for an Electrocatalyst*

The most desirable attributes for an electrocatalyst include high thermodynamic and kinetic stability, exceptional selectivity, and robust stability [39,40]. This study explores various methodologies employed in assessing the activity of an electrocatalyst. This study examines several commonly used parameters in electrochemistry, including overpotential at a specified current density, overpotential at a specified mass normalized current density, overpotential at a specified electrochemical surface area (ECSA), normalized current density, Tafel slope, exchange current density, and turnover frequency (TOF) [41].

The rate at which a reaction is taking place can be calculated by analyzing the last three of the aforementioned factors.

2.3. **Common Materials in Electrochemical Water-Splitting**

In recent years, extensive research efforts have been dedicated to the advancement of materials suitable for application as electrocatalysts [42][43]. The efficiency of hydrogen evolution through water electrolysis is contingent upon the utilization of a catalyst that possesses both stability and competence in reducing water at a low potential [44][45]. Hence, the primary objective is to decrease the catalyst's cost and enhance the energy conversion efficiency through modifications to the catalyst's composition [46]. Some commonly used materials are discussed below:

2.3.1. **Fe-based Metal Organic Framework (MOF)**

In recent years, there has been a significant increase in the interest surrounding materials based on Fe-MOFs. In addition to their utilization in electrochemical applications,

these materials have exhibited commendable efficacy in various other applications, including batteries, super capacitors, and CO₂ reduction methodologies. The exceptional performance of Fe-MOFs in the HER and OER, as well as their demonstrated versatility in terms of tunability, has been well-documented. Despite the progress made, significant advancements are still required before these innovations can be successfully brought to market. The synthesis of Fe-MOFs is characterized by a high degree of sensitivity, primarily due to the utilization of high-temperature pyrolysis as the predominant method. Consequently, there exists an increased probability of detrimental alterations occurring to the precursor of the MOFs during this process. The preservation of the Fe-MOF structure is crucial during the processes of HER and OER, given the absence of genuine electrochemically active sites on the structure. The material's ability to facilitate the reaction relies heavily on the metal nodes [47].

2.3.2. Transition Metal Carbides/Nitrides

The aforementioned class of electrocatalysts has exhibited exceptional conductivity, remarkable resistance to corrosion, notable stability, and distinctive electronic structures, thereby manifesting a remarkable efficacy in the process of water electrolysis. The existing body of research on these materials reveals a notable performance gap in comparison to benchmark catalysts, namely Pt, Ru, and Ir-based materials. The catalytic performance of Mo and W carbides/nitrides, along with NiMo and NiFe-based nitrides, has been extensively studied and proven to be highly effective in the process of water splitting. The unsatisfactory stability of these materials, however, remains a significant concern [48].

2.3.3. Transition Metal Selenides

The superior electrocatalytic performance of multi-metal selenides and their composites compared to single metal selenides has been observed within the realm of materials studied in this particular class. The issue of stability arises despite the excellent electrochemical performance exhibited by these materials. The durability of selenide-based materials in highly acidic or basic environments, as observed during the HER and OER, appears to be limited [49].

2.3.4. Activated Carbon based Materials.

Recently, a notable increase in interest towards carbon materials and their nanostructures is seen. The increased attention given to these materials can be attributed to their wide array of applications, which include storage of energy, sensing, and their use as electrocatalysts. The interest in these materials is primarily driven by their electrical

conductivity, chemical stability, and capacity to introduce electrochemically active species [50–52]. Activated carbons are widely recognized for their notable characteristics, including a substantial surface area, extensive microporosity, exceptional conductivity, affordability, and significant adsorption capacity. These attributes make them highly suitable for utilization as electrode materials [53].

2.3.5. Transition Metal Oxides

Transition-metal oxides, such as molybdenum trioxide (MoO_3), have received considerable interest within the area of HER because of their remarkable redox characteristics ($\text{Mn}^+ + \text{e}^- \rightarrow \text{Mn}^{\pm 1}$). For HER, the expedited electron transportation, facilitated by the distinctive configuration of these entities [54]. Many different MoO_3 morphologies have been studied that have shown promising results HER [55].

Summary

This chapter provides a comprehensive literature review of the study. It provides a comprehensive analysis of the advantages of utilizing hydrogen as a fuel source, in addition to an in-depth examination of the commonly employed techniques for hydrogen production. It provides a comprehensive analysis of electrochemical water-splitting as a viable method for hydrogen production, focusing on the elucidation of its reaction mechanisms. This study examines the various categories of materials commonly investigated for water-splitting, highlighting their respective advantages and limitations.

Chapter 3

Materials and Methods

3.1. Synthesis

3.1.1. Materials

Wheat straw (Agricultural waste originating from the regional fields in Pakistan.), KOH, NaOH (>99.0%, Sigma Aldrich), ethanol(>99.0%, Sigma Aldrich), and Ni Foam were all utilized in their received forms. To eliminate the nickel oxide layer, the Ni foam substrates estimating 1 x 1 cm² were exposed to treatment with a 3M HCl. After which, they were entirely washed and dried in stove at 60°C for 12 hours.

To guarantee the immaculateness of the wheat straw (WS) test, a surmised measure of 150g was estimated. The sample then, at that point, went through various intensive washings utilizing deionized water, cautiously eliminating any contaminations that may be available. This cautious cycle was completed to ensure the greatest amount of immaculateness of the Wheat Straw (WS) guaranteeing exact and dependable outcomes in resulting examinations. A while later, the material went through an intensive drying cycle to eliminate any overabundance dampness. It was then put away to be utilized as a precursor in the creation of Wheat Straw Charcoal (WSC). After the wheat straw had gone through the important pretreatment process, it was then cautiously grinded. These finely ground particles were then brought into a pyrolysis reactor, where pyrolysis process occurred. During the pyrolysis cycle, the material was heated to a continuous rise in temperature, at a pace of 2 °C each moment. This cautious and controlled heating went on until the material reached at a temperature of 450 °C. Subsequent to arriving at the ideal temperature, the material was painstakingly kept at this particular temperature for a time of 60 minutes. This temperature brought about the change of the WS into wheat straw char (WSC). After the wheat straw char had been painstakingly arranged, the time had come to make the following stride simultaneously. To guarantee that any debasements present were totally disposed of, the char, it went through a treatment involving a 1 M NaOH for a span of 30 minutes. This treatment was significant in guaranteeing that the eventual outcome would be liberated from any undesirable substances. Following this, char went through a progression of moves toward guarantee its quality. To accomplish this, the charcoal was exposed to different intensive washes utilizing deionized water. This cautious washing process disposed of any

pollutants or undesirable substances that might have been available in the charcoal. After the washing stage, the charcoal was then painstakingly dried to eliminate any excess dampness. This drying system was completed in a controlled climate in a broiler at a temperature of 100 °C. The charcoal was passed on to dry for a span of 12 hours, permitting plenty of time for the dampness to totally dissipate.

3.1.2. Making of Wheat Straw Activated Carbon WSAC

For activation, a painstakingly estimated measure of 5 g of Wheat straw char (WSC) was painstakingly blended in with a solution of potassium hydroxide (KOH). KOH concentration was of 40% by weight. The exact ratio of WSC to KOH was kept up at 1:5. The blend was then exposed to a mixing for 30 minutes. This guaranteed that every one of the parts were completely blended and uniformly dispersed inside the combination. After this underlying blending, the combination went through an extra move toward work on its homogeneity. To accomplish this, the blend was exposed to sonication for 30 extra minutes. This step was significant in guaranteeing the general quality and consistency of the combination. Following the sonication, the blend was then dried at temperature of 100 °C for 24 hours. After this, the powder was kept inside a tube furnace. This enactment cycle was done in a controlled environment. To establish this environment, nitrogen gas (N₂) was flown into the furnace, bringing about an inert environment. During this interaction, the material goes through a painstakingly controlled heating methodology. This includes exposing the material to a progressive rise in temperature, with a heating pace of 5 °C each moment. The cycle goes on till the material arrives at its final activation temperature of 800°C. Subsequent to arriving at the ideal temperature, the material was kept at this particular temperature for a term of one and a half hours. After this, the subsequent item was painstakingly exposed to a washing treatment. This treatment included the utilization of deionized (DI) water, which guaranteed that any impurities were taken out. The item was then dried in oven at a temperature of 100°C, permitting it to stay there for a term of 24 hours. The synthesized material was named AC.

3.1.3. Synthesis of MoO₃ Loaded Activated Carbon (MoO₃@AC)

For MoO₃ loaded Activated Carbon (AC) composite, a painstakingly estimated measure of MoO₃ was blended in with an equivalent amount of AC in 1:1 proportion. By using this proportion, the composite was intended to show upgraded properties and execution, using the qualities of both MoO₃ and AC. For this, deionized water (DI-water) was utilized. To accomplish a uniform blend, a stirrer was utilized. It assumed a significant part in blending the subsequent combination completely, ensuring homogeneity. By using this technique, we

accomplished the ideal consistency and guarantee that all parts were equally disseminated all through the solution. After this, the water was evaporated. After this, the MoO_3/AC composite was painstakingly kept it in an oven for drying overnight.

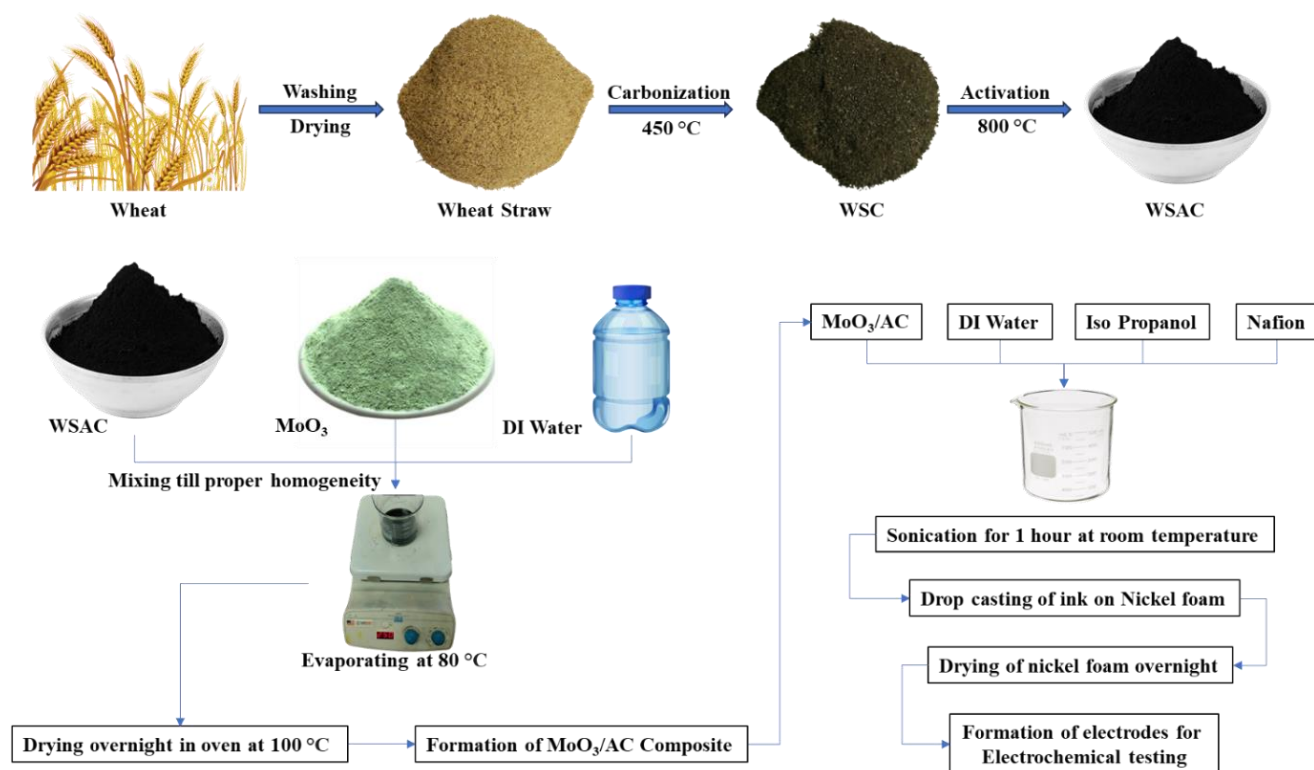


Figure 3.1: Schematic Diagram for electrocatalyst synthesis

3.2. Catalyst Characterization and Techniques Overview

3.2.1. X-Ray Diffraction (XRD)

In the realm of materials science, X-ray diffraction, often known as XRD, is a technique that is utilized frequently for the goal of determining the crystal structure of various substances. This method makes use of X-rays, the wavelength of which is comparable to the interatomic spacing that exists within the crystal lattice of a material. As a result, it is possible to determine the typical distance that exists between the atomic layers or rows that make up the crystal. This investigation makes use of a method that allows for the assessment of not only the size but also the shape of crystallites, as well as the alignment of grains or single-crystals [56]. The objective of this research is to explore a crystalline material by shining a beam of X-rays onto it, which will lead to the elastic dispersion of these X-rays as a result of the interaction. This dispersion takes place as a direct consequence of the periodic organization of the lattice structure. The dispersion of X-rays is a phenomena that results from the complex interaction between X-ray photons and the electrons that are found in the outermost shells of atoms. This interaction is

what causes the X-rays to spread out in all directions [57]. The phenomenon of diffraction is intricately elucidated by Bragg's law, which expounds upon the interrelationship between the wavelength of irradiated X-rays and the spatial separation of atoms:

$$2d\sin\theta = n\lambda$$

In the context of X-ray diffraction, the variables are defined as follows: d represents the perpendicular distance between neighboring atomic planes, θ denotes the incidence angle of X-rays at which diffraction occurs, λ represents the wavelength of the X-ray beam used for irradiation, and n signifies an integer denoting the order of reflection. The order of reflection is indicative of the path difference between scattered waves originating from adjacent atomic planes [56].

In addition to its primary applications, X-ray diffraction (XRD) can be employed for the estimation of average crystallite size. This is achieved through the utilization of the Scherrer equation, which considers the broadening of diffraction peaks:

$$t = K\lambda/\beta\cos\theta$$

In this study, we consider the relationship between the crystallite size (t), the Scherrer constant (K), the wavelength of the irradiating X-ray beam (λ), and the full width at half maximum of the diffraction peak (β). The Scherrer equation, while widely used for determining crystallite size from peak broadening in X-ray diffraction patterns, does not fully account for the presence of intrinsic crystallite defects and strains that can contribute to peak broadening. The determination of crystallite size through X-ray diffraction (XRD) should not be considered as an absolute measure. Therefore, it is crucial to support these findings with additional techniques like transmission electron microscopy (TEM) [56,57].

X-ray diffraction (XRD) is a versatile technique that enables the assessment of various aspects related to a mixture's elemental composition, the deviation of a specific crystalline material from its ideal structure and composition, as well as the crystallinity of the material [58].

3.2.2. Scanning Electron Microscopy (SEM)

The method known as scanning electron microscopy (SEM) utilizes an electron shaft that is firmly engaged to produce high-resolution pictures of the outer layer of a material. This innovation is fit for achieving an high resolution of up to 1 nanometer [59]. With regards to

electron microscopy, we notice a wide range of peculiarities that happen in view of the collaboration between the electron shaft and the material's surface that we're considering. Other than creating three distinct sorts of signals, these attributes additionally include emitting X-rays that can be effortlessly separated from one another. The signs are made out of three fundamental sorts of electrons: primary electrons, secondary electrons, and Auger electrons. Primary electrons collaborate with the sample and experience flexible backscattering, while secondary electrons associate with the sample and go through inelastic backscattering. These three sorts of electrons by and large add to the signs noticed. To make definite pictures of the example's surface, we can utilize a method that includes secondary electrons or electrons that have been backscattered. This procedure assists us with catching high-resolution pictures. By utilizing different X-rays and utilizing the energy dispersive X-ray examination (EDX) innovation, it becomes more straightforward to recognize the components present in an example. Moreover, Auger electrons plays a vital part in surface examination techniques [56,58].

To guarantee accurate imaging, it is significant for the sample utilized in scanning electron microscopy (SEM) to have electrical conductivity. If this necessity isn't met, it could make electrostatic charge expand on the sample's surface, possibly causing picture distortion. To resolve this issue actually, it is vital that the example shows conductivity and is appropriately grounded. To upgrade conductivity, samples that need conductivity are covered with a layer of gold. To guarantee the best picture clearness, it is pivotal for sample to be totally absent of any water. The justification for this is that scanning electron microscopy (SEM) works in a high vacuum environment. This can make water evaporate, which thus can influence the nature of the subsequent pictures [57].

3.2.3. Raman Spectroscopy

Krishnan and Raman created Raman spectroscopy in 1928. By modifying the polarizability of molecules, it offers information about the sample [60]. Raman spectroscopy is a potent analytical method for samples in liquid, solid, and gas phases. This approach gives dependable information on the sample's structural and chemical characteristics. It is employed in the sectors of energy, pharmaceuticals, forensics, and biomedicine [61].

3.2.3.1. Working Principle

Raman spectroscopy detects the signal produced by the sample's inelastic scattering of radiation. Light photons are dispersed when UV-Vis or IR radiation is projected across a

material. These photons captured by lenses are focused on a detector to form a Raman spectrum. As a consequence of the radiation's interaction with the sample, the frequency of the photons that are entering the system might or might not change. Radiation that has been absorbed may then be radiated at the same or different frequencies. The phenomenon known as Rayleigh scattering takes place whenever transmittance takes place at the same frequency. On the other hand, the phenomenon known as Raman scattering takes place whenever transmittance is not elastic and there is a change in the frequency of the emitted photon, as indicated in the figure. Raman scattering can be further classified as follows:

- Stokes scattering (reduction in frequency of emitted photon)
- Anti-Stokes scattering (increment in frequency of emitted photon) Scattering of photons provides information about vibrational, rotational changes in samples [62].

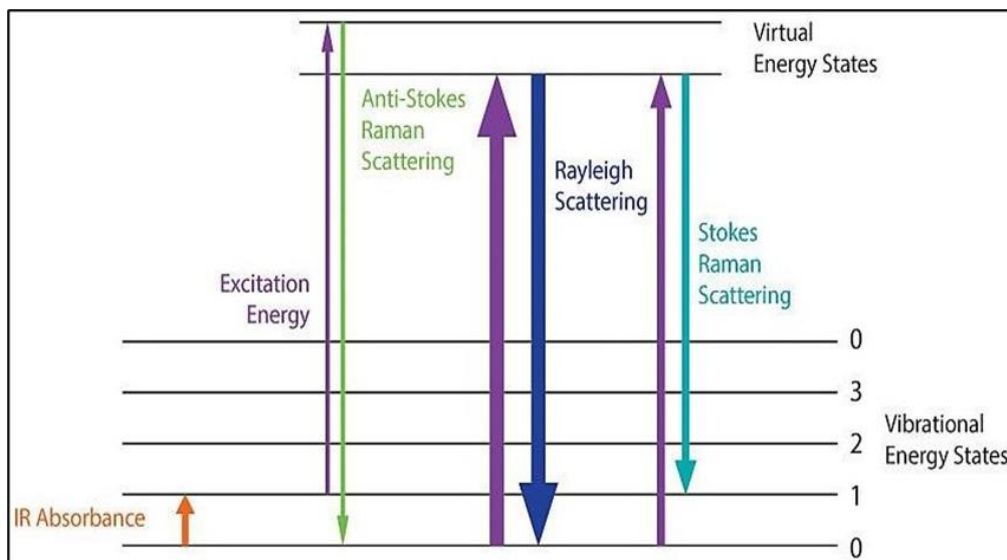


Figure 3.2: Energy level diagram in Raman spectroscopy

3.2.3.2. Instrumentation

Figure 15 shows the essential components of Raman spectrophotometer, which includes:

- Radiation source
- Sample holder
- Lenses system
- Detectors

- Computer control

Arrangement and replacement of these components could be different in different kind of Raman spectrophotometer [63].

3.2.4. N₂ Adsorption – Desorption

The measurement of a material's surface area is commonly conducted through the utilization of N₂ adsorption-desorption techniques. This study examines the phenomenon of adsorption and desorption of N₂ on the surface of a sample. Adsorption is observed to take place at low temperatures, wherein N₂ molecules are physically adsorbed onto the sample's surface. Conversely, desorption is observed at high temperatures, wherein N₂ molecules detach from the surface of the sample. The surface of the sample has the capability to adsorb N₂, resulting in the formation of either a monomolecular or multimolecular layer. The physical nature of adsorption renders it non-selective, as evidenced by the fact that N₂ would adsorb onto the surface of any sample at its boiling point [64].

The assessment of surface area in samples is commonly conducted using the Brunauer-Emmett-Teller (BET) model, which relies on the analysis of adsorption-desorption isotherms. The determination of the quantity of N₂ adsorbed can be achieved by adjusting the pressure of N₂ after reaching equilibrium during analysis. The replication of calculations at various N₂ pressures allows for the acquisition of an adsorption isotherm, which serves as a valuable tool in the determination of pore size, pore volume distribution, and surface area of the sample. The estimation of pore size and pore volume distribution is a common application of the Barrett-Joyner-Halenda (BJH) model [65].

3.3. Experimental Setup for Electrochemical Measurements

The electrochemical measurements in this study were done utilizing a CH Instruments Model 660E Electrochemical Workstation, which is an advanced equipment that can do extremely correct and exact measurements and analysis. It was equipped with a three-cathode assembly, which is used for electrochemical testing. Ag/AgCl was utilized as the reference cathode and platinum wire was utilized as the counter electrode and a working electrode made of nickel foam were used.



Figure 3.3: Electrochemical workstation setup

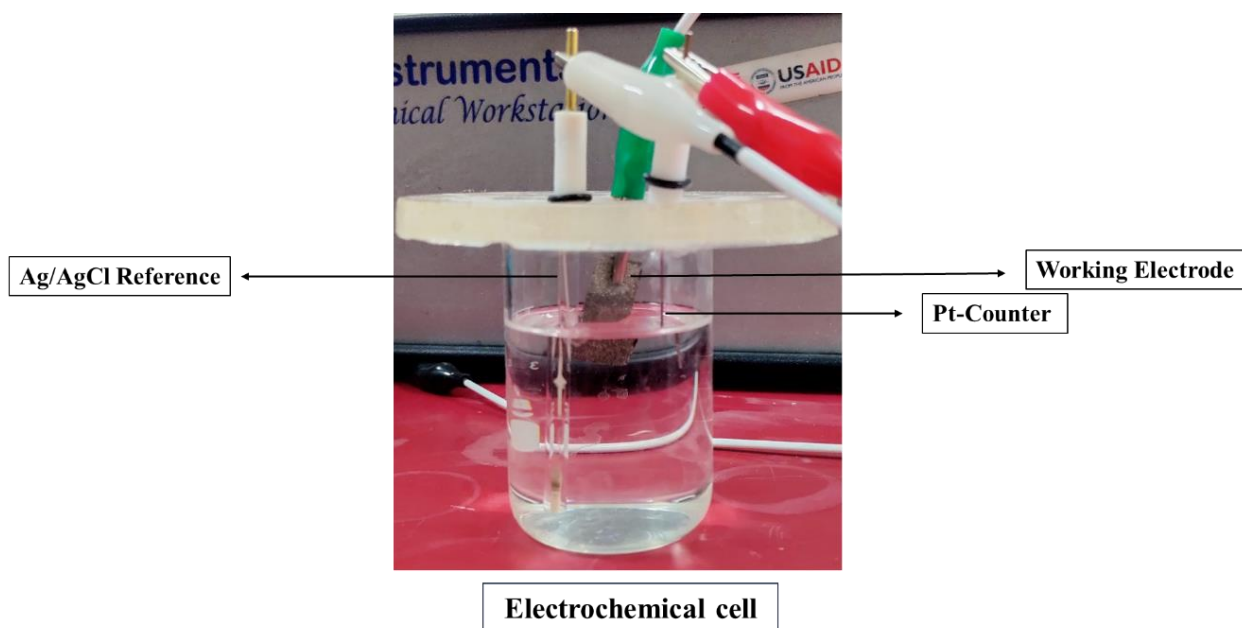


Figure 3.4: Three Electrodes System

In this study, a three electrode assembly was used for the testing and analysis, wherein the Ag/AgCl was utilized as the reference cathode and platinum wire was utilized as the counter electrode and a working electrode made of nickel foam were used. The nickel foam substrate was treated in a solution of 3 M hydrochloric acid (HCl), followed than by sonication in DI

water, and at last sonication in ethanol. Every treatment went on for a span of 15 minutes. After this the Ni foam substrates were dried at 60 °C for 2 hours, guaranteeing ideal circumstances for the evacuation of any remaining moisture. The ink detailing included the mix of 15 mg of active material, 3 mg of carbon black, and 2 mg of PVDF in a 100 μL of NMP. For proper dispersion, it was sonicated overnight. In this study, the ink was drop projected onto a 1x1 cm² nickel foam substrates. Then dried at a temperature of 60 °C for a span of 3 hours. In this study, the electrochemical measurements of different electrocatalysts were carefully analyzed. The analysis were done in a 0.5 M KOH solution, with the scan rates being changed systematically. The tests directed for each example incorporated the assessment of the OER, HER, cyclic voltammetry (CV), and impedance spectroscopy (EIS). The use of the reversible hydrogen electrode (RHE) potential was utilized for resulting computations. In this study, the equation used to determine RHE potential values at a pH of 14 is [66]:

$$E_{RHE} = E_{Ag/AgCl} + 0.059pH + 0.1976$$

Summary

The chapter gives a far-reaching idea on the approach for the synthesis of the material that was used in the analysis. This study gives an extensive idea on the techniques for portrayal that were used for the assurance of the material's properties. The accompanying part gives a thorough stock of the instruments that were used, as well as the parameters that were collected from each instrument. Furthermore, the equations that were used for calculations are added.

Chapter 4

Results and Discussion

4.1. Physicochemical Properties of the Electrocatalyst

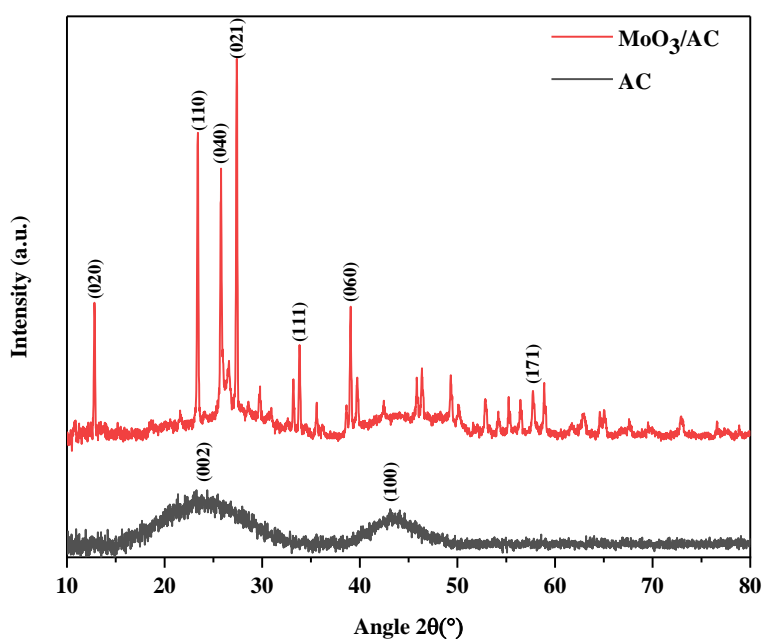


Figure 4.1: XRD of AC and MoO₃@AC

Based on the XRD spectra presented in Figure 4.1, the activated carbon sample exhibits two distinct diffraction peaks spanning the 2θ range of 20-30 and 40-50. These peaks indicate that amorphous carbon is present, characterized by a disordered arrangement of carbon rings. An amorphous structure is exhibited by the AC sample, with a significant presence of microcrystals displaying a turbostratic graphite arrangement. X-ray diffraction investigation showed two different diffraction peaks, one for microcrystalline graphite and one for turbostratic graphite, which correspond to the (002) and (100) crystal faces, respectively. The diffraction spectrum obtained from the activated carbon sample exhibits the presence of a microcrystalline crystal face, specifically the (002) plane, as depicted in Figure 4.1. Based on the application of Bragg's equation, $2d\sin\theta = n\lambda$, it is evident that the plane spacing 002, of the diffraction crystal face (002) in the activated carbon sample is comparatively larger. This observation suggests that the activated carbon prepared exhibits a relatively prominent

turbostratic degree [67]. The (100) crystal surface peak exhibited a gentler profile. Additionally, the diffraction peaks were observed at $2\theta = 43.98$, and it was observed that the diffraction peak was stronger in intensity. The X-ray diffraction (XRD) pattern of the $\text{MoO}_3@\text{AC}$ sample displayed distinct peaks that can be attributed to the presence of MoO_3 , as indicated by the JCPDS No. 05-0508 reference. The diffraction peaks located at 13° , 23.3° , 25.7° , 27.3° , 34° , 39° , and 58° were identified to correspond to the crystallographic planes (020), (110), (040), (021), (111), (060), and (171) of MoO_3 , respectively.

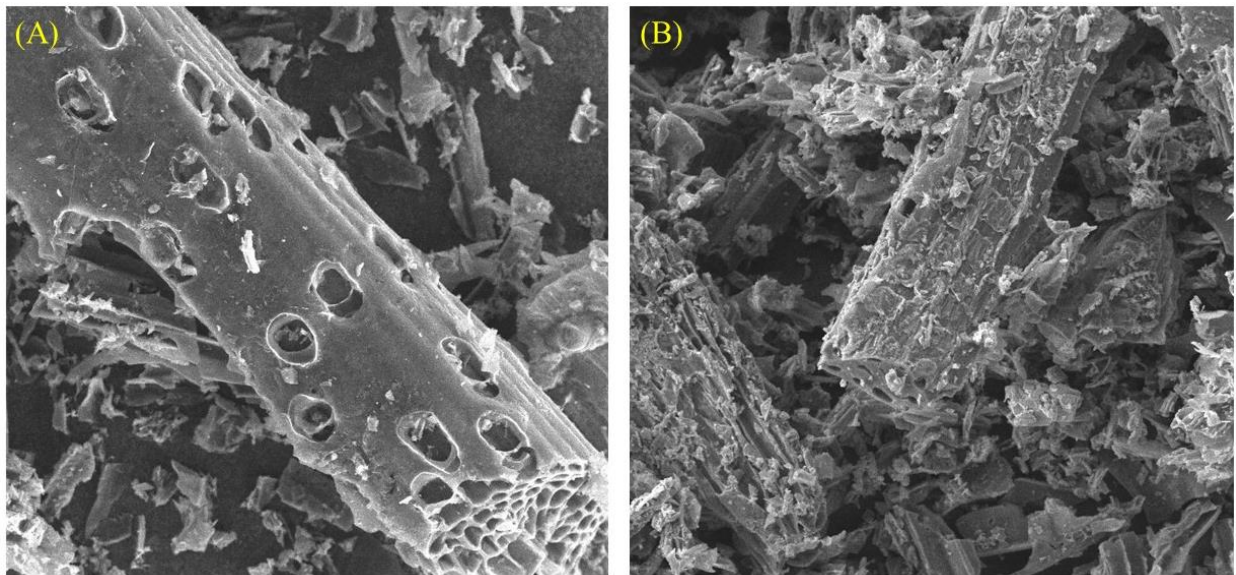


Figure 4.2: SEM images of (A) AC at 50 μm and (B) $\text{MoO}_3@\text{AC}$ at 50 μm

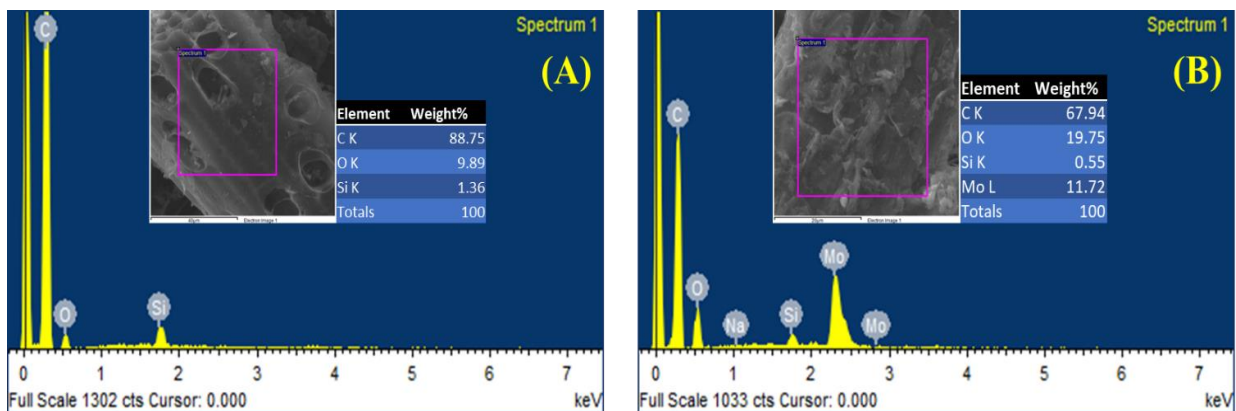


Figure 4.3: EDS of (A) AC and (B) $\text{MoO}_3@\text{AC}$

Fig. 4.2-A depicts SEM image, demonstrating existence of void tunnels within the activated carbon sample. It is postulated that these tunnels have been generated through the process of activation, wherein the gasification of volatile substances present inside the samples occurs [68]. Figure 4.2-B depicts a visual representation of the scanning electron microscopy (SEM) picture illustrating the composite material composed of AC and MoO_3 in a 1:1 ratio.

The morphological properties observed in both AC and MoO₃ are exhibited by the composite resulting from their combination. The structural properties of AC and MoO₃@AC samples are clearly distinguished in the scanning electron microscopy (SEM) pictures. The AC structure demonstrates a heightened level of porosity prior to the implementation of MoO₃ onto its surface. However, subsequent to the introduction of MoO₃, the porousness of the AC framework diminishes, which aligns with the observations made during the Brunauer-Emmett-Teller (BET) analysis. Figure 4.3 displays the results of elemental analysis conducted on the synthesized samples, namely AC and MoO₃@AC. As seen from the figure 4.3, the presence of Mo is clearly observed, along with a noticeable rise in the weight percentage of oxygen.

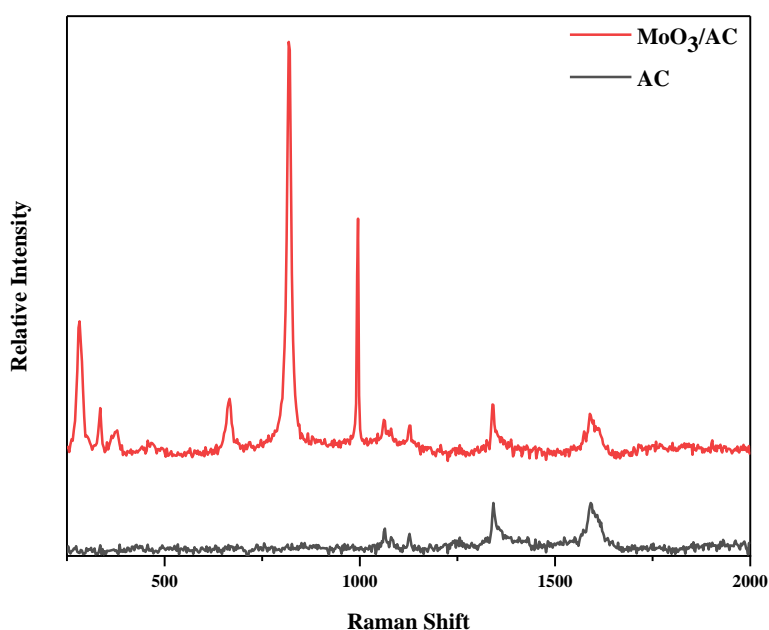


Figure 4.4: Raman Spectra of AC and MoO₃@AC

The Raman spectrum provides evidence of the molecular vibration and rotation characteristics of AC and MoO₃@AC in a thorough manner. The D band and G band exhibit peak frequencies at 1342 cm⁻¹ and 1591 cm⁻¹, respectively. The spectral characteristic observed at 1342 cm⁻¹, known as the D band, is commonly associated with the existence of regions containing disordered and structurally defective sp³-hybridized carbon atoms. On the other hand, the G band, which is detected at a wavenumber of 1591 cm⁻¹, is linked to the elongation of the carbon-carbon double bond (C=C) within graphitic carbons that exhibit sp² hybridized carbon systems. In the case of MoO₃, it is evident that a discernible peak is detected at a wavenumber of 380 cm⁻¹, which can be ascribed to the scissoring oscillation of the oxygen-

molybdenum-oxygen (O–Mo–O) chemical bonds. Furthermore, an additional peak is detected at a wavenumber of 335 cm⁻¹, which can be attributed to the bending motion of the O–Mo–O bonds. Additionally, a detected peak at a wavenumber of 282 cm⁻¹ suggests the presence of the wagging motion in the oxygen-molybdenum-oxygen (O=Mo=O) bonds. Furthermore, the peaks seen at a wavenumber of 666 cm⁻¹ can be ascribed to the stretching of O–Mo–O bonds, while the peaks at 818 cm⁻¹ and 995 cm⁻¹ can be associated with the stretching of terminal Mo=O bonds, respectively [69,70].

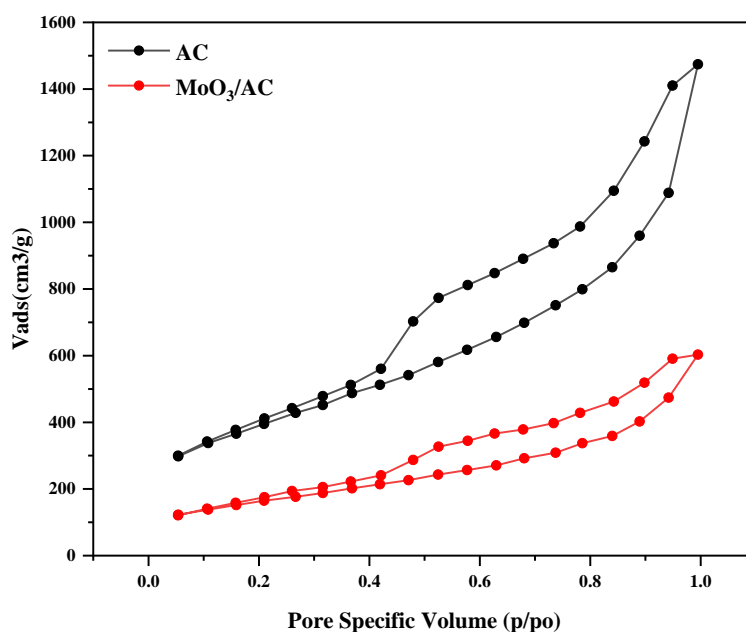


Figure 4.5: N₂ Adsorption-Desorption Isotherm

Table 4.1: Summary of N₂ Adsorption-Desorption

Catalyst	Specific Surface Area	BJH Adsorption Pore Volume (cm ³ /g)	BJH Pore Diameter (nm)
AC	1367.571 m ² /g	1.854 cm ³ /g	4.0366 nm
MoO ₃ @AC	565.884 m ² /g	0.759 cm ³ /g	4.0968 nm

The investigation of the textural qualities was conducted using the Barrett-Joyner-Halenda (BJH) method. The results of this investigation demonstrate that the incorporation of MoO₃ led to a decrease in micropore volume, declining from 1.854 cm³/g to 0.759 cm³/g when nitrogen was employed for aeration. The inclusion of MoO₃ resulted in a significant decrease in volume of micropores. The surface area of the activated carbon (AC) and the AC impregnated with MoO₃ (MoO₃@AC) was measured to be 1367.571 m²/g and 565.884 m²/g, respectively. The observed reduction in surface area can be attributed to the presence of MoO₃ on the activated carbon (AC) that was produced. This presence effectively filled the pores

inside the AC material. The aforementioned finding is supported by the scanning electron microscope (SEM) images obtained.

Fig. 4 displays the isotherms pertaining to the adsorption and desorption processes of nitrogen (N₂) on activated carbon (AC) and molybdenum trioxide supported on activated carbon (MoO₃@AC). The isotherms observed for both the AC and MoO₃@AC catalysts exhibit Type IV behavior, as specified by the IUPAC. Additionally, H4 hysteresis loops are observed in both cases.[71]. The slender mesoporous pore structures of the investigated electrocatalysts were seen to be produced in a slit-like configuration. The occurrence of hysteresis loop can be attributed to the phenomenon of capillary condensation taking place within mesopores, which is triggered by an increase in relative pressure [71] As can be seen in table-1 above, AC has a larger surface area than MoO₃@AC, resulting in a longer hysteresis loop.

4.2. Electrocatalysts Electrochemical Performance

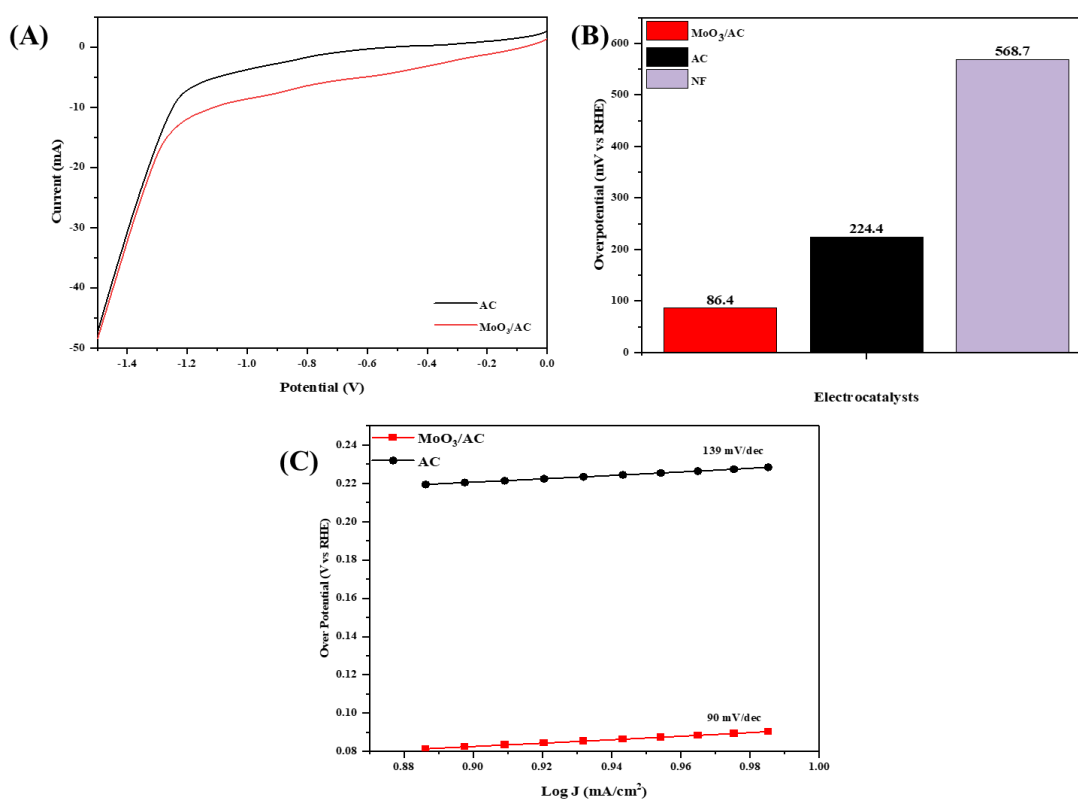


Figure 4.6: (A) HER (LSV Curves), (B) MoO₃@AC, AC and NF Overpotentials, (C) Tafel plots for HER

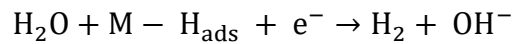
LSV polarization curves were used to probe the HER in AC and MoO₃@AC. These samples results were measured against those of bare nickel foam, which has been shown to

have a suitable level of activity in HER (i.e. 568.7 mV), for comparison [30]. Upon analyzing the data, it becomes evident that the MoO₃@AC sample demonstrates enhanced performance in comparison to the AC sample. This is supported by the MoO₃@AC sample's lower overpotential of 86.4 mV and a Tafel slope of 90.2 mV/dec, whereas the AC sample exhibits an overpotential of 224.4 mV and a Tafel slope of 139 mV/dec. The Volmer-Heyrovsky steps are utilised to describe the mechanism that underlies the HER [13].

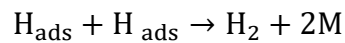
Adsorption step (Volmer reaction)



Desorption step (Heyrovsky reaction)



Desorption step (Tafel reaction)



Here M represents the active sites. The alkaline solution is responsible for the formation of the adsorbed hydrogen intermediate by the mechanism of water molecule discharge. Hydrogen gas (H₂) is then released after a desorption process [66].

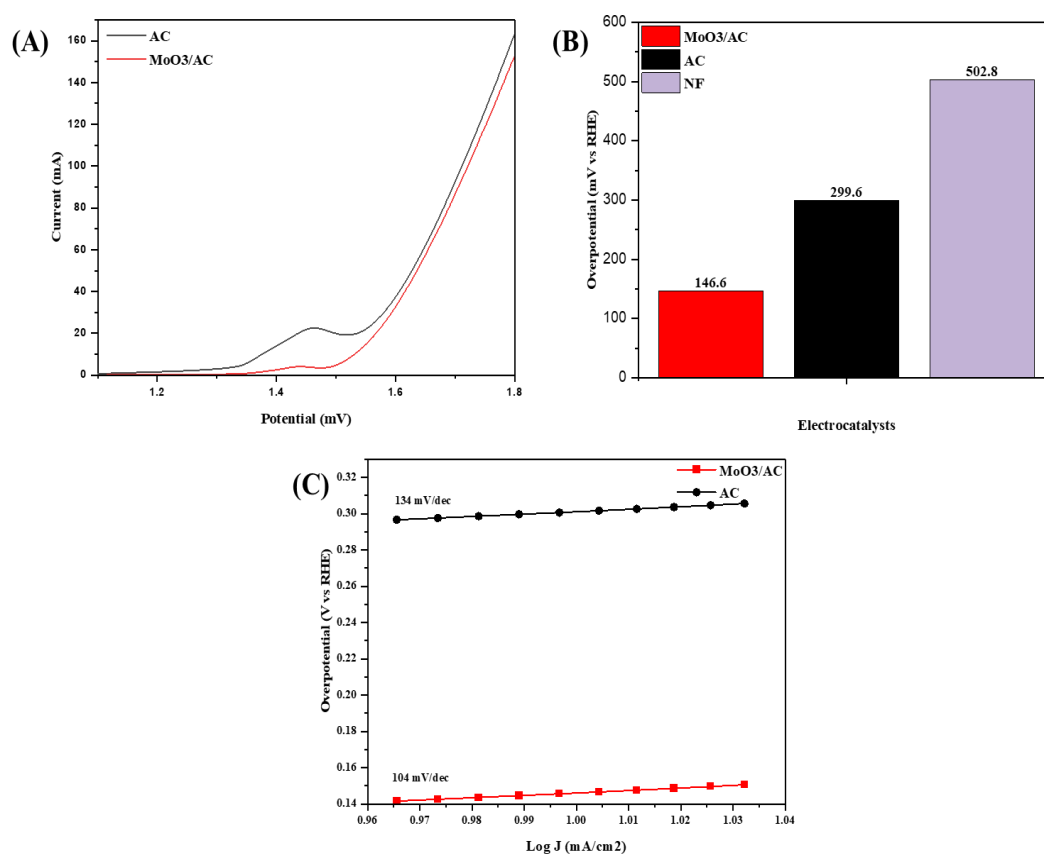


Figure 4.7: (A) OER (LSV curves), (B) MoO₃@AC, AC and NF (Overpotentials), (C) Tafel plots for OER

Linear Sweep Voltammetry (LSV) polarization curves were used to assess the OER performance of AC and MoO₃@AC. The data presented in Figure 4.7 demonstrates that the MoO₃@AC composite exhibits superior performance compared to the base AC sample, as evidenced by its significantly lower overpotential of 146.6 mV, in contrast to the 299.6 mV for AC. The aforementioned observation is supported by the data, which reveals that MoO₃@AC demonstrates the lowest slope of 104 mV/dec, as determined through Tafel plot analysis. In addition, it is worth noting that the electrocatalysts under investigation have been evaluated in comparison to the performance of the bare nickel foam, which exhibits a decent overpotential of 502.8mV in the OER [30].

Figure 4.8 (A) and (B) depicts the cyclic voltammetry (CV) curves for AC and MoO₃@AC, respectively, acquired at a scan rate of 10 mV/s. The Cyclic Voltammetry experiment yielded a quasi-rectangular curve for AC due to its inherent characteristics [72,73] and In the case of MoO₃@AC, clear redox peaks were observed, as evident from the obtained results.

The improved electrocatalytic performance of the catalyst can be attributed to the incorporation of MoO₃ within the pores of the synthesized activated carbon (AC), as evidenced by the scanning electron microscopy (SEM) images depicted in Fig. 2. This hypothesis is supported by the BET results, which indicate a decrease in surface area for the resulting composite MoO₃@AC compared to the pristine AC.

The kinetics of the synthesized electrocatalysts were investigated using electrochemical impedance spectroscopy (EIS) measurements, as depicted in Figure 4.8(C). The experiment encompassed a range of frequencies from 100 mHz to 1000 kHz, with an applied voltage of 10 mV. The above graph depicts the constituent elements of a comparable electrical circuit. The letter R₁ or R_S is used to represent the electrolyte's ohmic resistance existing between the electrodes. The polarization-opposing force at the electrode–electrolyte interface is represented by the charge transfer resistance, R₂ or R_{CT}. In addition, W represents the Warburg's impedance, and the faradic capacitance is shown by the sign C₁. Table 2 displays the computed resistances of each sample.

Table 4.2: Resistances for AC and MoO₃@AC obtained from EIS.

Sample ID	R_S (Ω)	R_{CT} (Ω)
AC	1.315	24.89
MoO₃@AC	1.193	7.333

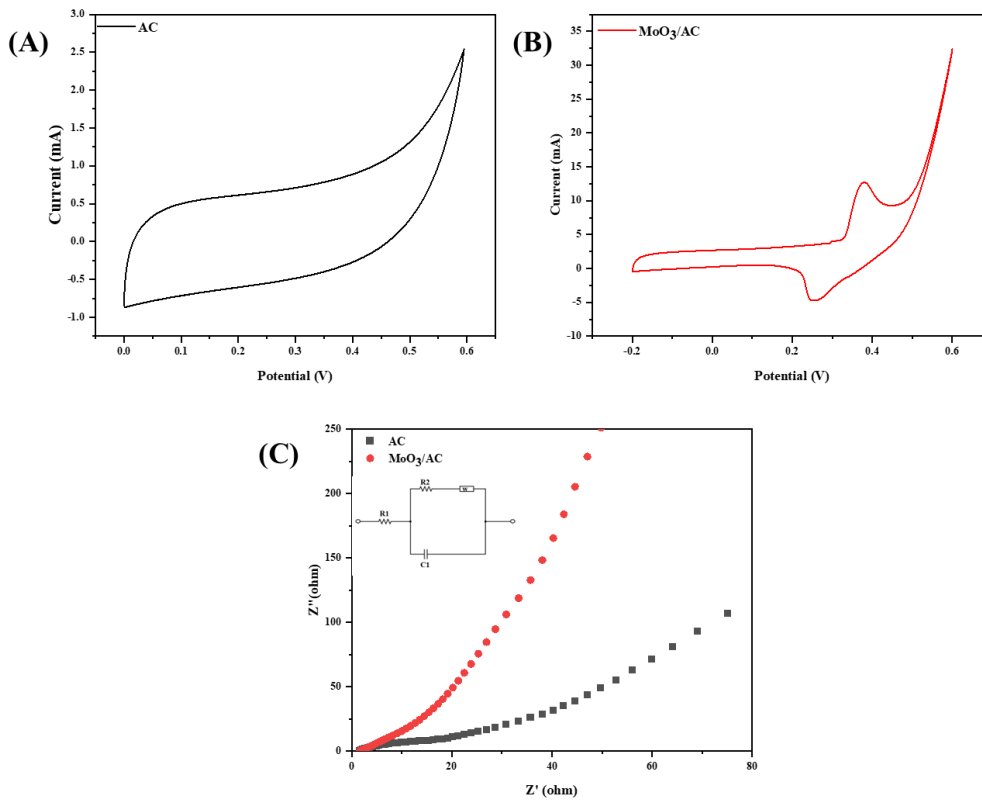


Figure 4.8: (A) CV for AC, (B) CV for MoO₃@AC, (C) EIS for AC and MoO₃@AC

Table 4.3: Comparison of recent studies conducted on AC and MoO₃ with the synthesized electrocatalysts

Catalyst	HER	Tafel Slope	OER	Tafel Slope	References
AC	86.4	90	146.6	104	This Work
MoO ₃ @AC	224.4	139	299.6	134	This Work
NiOx-AC-450	277	133.8	383	111.4	[74]
NiFe/MoO ₃ @CFP	204	106	251	78	[75]
Ni ₃ N/Ru/NCAC	42	59	288	60	[76]
Ti ₃ C ₂ @ MoO ₃	91	34	190	59	[77]
NMWNT	340	-	320	68	[78]

Summary

This chapter provides a comprehensive presentation of the findings as well as an in-depth analysis of the results. The techniques of characterization are initially utilised in order to provide information on the physiochemical properties of the electrocatalysts. The electrochemical performance of the catalysts that are utilised for the process of water splitting has been presented, discussed, and compared with the findings of recent investigations.

Chapter 5

Conclusions and Recommendations

5.1. Conclusions

Water splitting is widely regarded as a highly reliable and promising technological approach to effectively tackle environmental challenges and provide a sustainable means of energy conversion. Numerous investigations have been conducted on various metal oxides, carbides, and sulphides in relation to their performance in the HER and OER. However, it is important to note that each of these materials demonstrates distinct characteristics and kinetics in terms of their HER and OER capabilities. Achieving a significant level of catalytic activity for bifunctional catalysts, which exhibit diverse kinetics for OER and HER, while simultaneously addressing challenges related to inadequate conductance and charge transfer, represents a challenging and very time-consuming endeavor. Numerous electrocatalysts have been developed and studied extensively in the context of HER and OER with the aim of achieving exceptional performance in electrocatalytic water splitting. The researchers are currently engaged in the development of a bifunctional catalyst that exhibits a notable energy conversion efficiency while also demonstrating a minimal overpotential. The efficacy of bifunctional heterostructure catalysts has been proven in the processes of HER and OER, which are crucial for hydrogen generation as a fuel source. In light of this, a bifunctional electrocatalyst composite, MoO₃@AC, was synthesized with a 1:1 ratio of MoO₃ to AC. The optimized sample exhibited significant HER and OER activity, with minimal overpotentials of 86.4 mV and 146.6 mV, respectively. The enhanced HER (hydrogen evolution reaction) and OER (oxygen evolution reaction) performance of MoO₃@AC, in comparison to AC alone, can be attributed to the inclusion of MoO₃ within the pores of AC. This inclusion facilitates the transit of electrons and charges, as evidenced by the SEM images and BET (Brunauer-Emmett-Teller) data, thereby supporting this idea. Due to the catalyst's exceptional performance, it possesses the potential to be advantageous in a diverse range of practical applications. This study paves the path for the development of bifunctional materials that can be utilised in the comprehensive process of water splitting. Therefore, more investigation into design methodologies and reaction mechanisms is important to develop an enhanced and more efficient catalyst that is also feasible in practical applications.

5.2. Recommendations

It is of the utmost importance that more research be carried out in order to evaluate the efficiency of the synthesized catalyst in the electrocatalytic water splitting process. Following are some recommendations for further research:

1. More exploration should be carried out on MoO₃-based catalysts and AC-based catalysts that are blended in with different materials, for example, perovskites.
2. One significant area of concentration in this field is the effective improvement of catalyst recovery.
3. These materials may be useful for something other than water splitting in electrochemistry i.e., batteries and supercapacitors.
4. Further insight into the effect of these variables on the performance of this electrocatalyst could be gained by studying the effect of modifying parameters including the electrolyte, substrate, and ink preparation procedures.

References

- [1] Tang X. Depletion of fossil fuels and anthropogenic climate change — A review 2013;52:797–809. <https://doi.org/10.1016/j.enpol.2012.10.046>.
- [2] Edition S. Principles energy systems. n.d.
- [3] Verne J. The Mysterious Island 1888.
- [4] Abe JO, Popoola API, Ajenifuja E, Popoola OM. ScienceDirect Hydrogen energy , economy and storage : Review and recommendation. Int J Hydrogen Energy 2019. <https://doi.org/10.1016/j.ijhydene.2019.04.068>.
- [5] Å RS. The hydrogen economy , fuel cells , and electric cars 2003;25:455–76. <https://doi.org/10.1016/j.techsoc.2003.09.024>.
- [6] Resources E. Fallacies of a Hydrogen Economy: A Critical Analysis of Hydrogen Production and Utilization 2016. <https://doi.org/10.1115/1.1804193>.
- [7] You B, Tang MT, Tsai C, Abild-pedersen F, Zheng X, Li H. Enhancing Electrocatalytic Water Splitting by Strain Engineering Enhancing Electrocatalytic Water Splitting by Strain Engineering 2019. <https://doi.org/10.1002/adma.201807001>.
- [8] Yin J, Jin J, Lin H, Yin Z, Li J, Lu M, et al. Optimized Metal Chalcogenides for Boosting Water Splitting 2020;1903070. <https://doi.org/10.1002/adv.201903070>.
- [9] Morales-guio CG, Stern L, Hu X, Stern L. Chem Soc Rev Nanostructured hydrotreating catalysts for electrochemical hydrogen evolution. Chem Soc Rev 2014;43:6555–69. <https://doi.org/10.1039/C3CS60468C>.
- [10] You B, Tang MT, Tsai C, Abild-pedersen F, Zheng X, Li H. Enhancing Electrocatalytic Water Splitting by Strain Engineering 2019;1807001:1–28. <https://doi.org/10.1002/adma.201807001>.
- [11] Li Y, Wang H, Xie L, Liang Y, Hong G, Dai H. the HER2011;7296–9.
- [12] Recent advances and prospective in ruthenium- based materials for electrochemical water splitting 2019. <https://doi.org/10.1021/acscatal.9b02457>.
- [13] Sun H, Xu X, Song Y, Zhou W, Shao Z. Designing High-Valence Metal Sites for Electrochemical Water Splitting 2021;2009779:1–44.

- <https://doi.org/10.1002/adfm.202009779>.
- [14] Generation O, Status C. Water Splitting as an Alternative for Electrochemical Hydrogen and Challenges 2023.
- [15] Fiegenbaum F, Trombetta F, Martini EMA. ScienceDirect PtNi and PtMo nanoparticles as efficient catalysts using TEA-PS . BF₄ ionic liquid as electrolyte towards HER Dem 2016:4–11.
- [16] Li Y, Sun Y, Qin Y, Zhang W, Wang L, Luo M. Recent Advances on Water-Splitting Electrocatalysis Mediated by Noble-Metal-Based Nanostructured Materials 2020;1903120:1–20. <https://doi.org/10.1002/aenm.201903120>.
- [17] Miles MH, Thomason MA. Periodic Variations of Overvoltages for Water Electrolysis in Acid Solutions from Cyclic Voltammetric Studies n.d.:1459–61.
- [18] Hu S, Feng C, Wang S, Liu J, Wu H, Zhang L, et al. Ni₃N / NF as bifunctional catalysts for both hydrogen generation and urea decomposition 2019. <https://doi.org/10.1021/acsami.8b19052>.
- [19] Zhao W, Wang S, Feng C, Wu H, Zhang L, Zhang J. Energy , Environmental , and Catalysis Applications xSe) as High Active and Stable Electrocatalysts for HERin Electrolysis Water Splitting Active and Stable Electrocatalysts for HERin 2018:0–33. <https://doi.org/10.1021/acsami.8b12797>.
- [20] Sharma S, Basu S, Shetti NP, Nadagouda MN, Aminabhavi TM. Microplastics in the environment : Occurrence , perils , and eradication. Chem Eng J 2021;408:127317. <https://doi.org/10.1016/j.cej.2020.127317>.
- [21] Sharma S, Basu S, Shetti NP, Kamali M, Walvekar P, Aminabhavi TM. Waste-to-energy nexus : A sustainable development *. Environ Pollut 2020;267:115501. <https://doi.org/10.1016/j.envpol.2020.115501>.
- [22] Manuscript A. ChemComm 2019. <https://doi.org/10.1039/C9CC01433K>.
- [23] Turner JA, Turner JA. Sustainable Hydrogen Production 2014;972. <https://doi.org/10.1126/science.1103197>.
- [24] Lv H, Geletii Y V, Zhao C, Vickers JW, Zhu G, Hill CL. Chem Soc Rev Polyoxometalate water oxidation catalysts and the production of green fuel w

- 2012:7572–89. <https://doi.org/10.1039/c2cs35292c>.
- [25] Zou X, Ott S. Electrocatalytic Hydrogen Evolution from a Cobaloxime-Based Metal – Organic Framework Thin Film 2019. <https://doi.org/10.1021/jacs.9b07084>.
- [26] Article R, Reza S, Yun CS, Afroze S, Radenahmad N, Bakar MSA, et al. Latest development of double perovskite electrode materials for solid oxide fuel cells : a review. Arab J Basic Appl Sci 2019;13:2004–13. <https://doi.org/10.1002/ange.202011069>.
- [27] Afroze S. Hydrogen Production from Water Splitting through Photocatalytic Activity of Carbon-Based Materials 2022:1–16. <https://doi.org/10.1002/ceat.202100513>.
- [28] Reza S, Yun CS, Afroze S, Radenahmad N, Bakar MSA, Saidur R, et al. Preparation of activated carbon from biomass and its ' applications in water and gas purification , a review. Arab J Basic Appl Sci 2020;27:208–38. <https://doi.org/10.1080/25765299.2020.1766799>.
- [29] Reza S, Ahmed A, Caesarendra W, Bakar MSA, Shams S, Saidur R, et al. Acacia Holosericea : An Invasive Species for Bio-char , Bio-oil , and Biogas Production 2019.
- [30] Sarmad Q, Masood U, Mahmood M, Hassan M, Ahmed F, Hussain A, et al. Journal of Environmental Chemical Engineering Praseodymium-doped Sr₂TiFeO_{6-δ} double perovskite as a bi-functional electrocatalyst for hydrogen production through water splitting. J Environ Chem Eng 2022;10:107609. <https://doi.org/10.1016/j.jece.2022.107609>.
- [31] Nikolaidis P, Poullikkas A. A comparative overview of hydrogen production processes. Renew Sustain Energy Rev 2017;67:597–611. <https://doi.org/10.1016/j.rser.2016.09.044>.
- [32] Blue, green, gray: the colors of hydrogen n.d.
- [33] Li F, Yang H, Zhuo Q, Zhou D, Wu X, Zhang P. Forschungsartikel A Cobalt @ Cucurbit [5] uril Complex as a Highly Efficient Supra- molecular Catalyst for Electrochemical and Photoelectrochemical Water Splitting Forschungsartikel 2021:2004–13. <https://doi.org/10.1002/ange.202011069>.
- [34] Zhang T, Sun J. Self-supported transition metal chalcogenides for oxygen evolution 2023.

- [35] Yu J, He Q, Yang G, Zhou W, Shao Z, Ni M. Recent Advances and Prospective in Ruthenium-Based Materials for Electrochemical Water Splitting 2019. <https://doi.org/10.1021/acscatal.9b02457>.
- [36] Manuscript A. Energy & Environmental Science 2017:0–10. <https://doi.org/10.1039/C7EE02537H>.
- [37] Sangeetha DN, Holla RS, Ramachandra B. ScienceDirect High power density and improved H₂ evolution reaction on MoO₃ / Activated carbon composite. Int J Hydrogen Energy 2019. <https://doi.org/10.1016/j.ijhydene.2019.10.029>.
- [38] Reaction HE, Li Y, Deng S, Shen S, Pan G, Xiong Q, et al. Accepted Manuscript n.d. <https://doi.org/10.1002/celc.201900448>.
- [39] Shi Y, Zhang B. Chem Soc Rev Recent advances in transition metal phosphide nanomaterials: synthesis and applications in. Chem Soc Rev 2016. <https://doi.org/10.1039/C5CS00434A>.
- [40] Electrocatalysts N, Katsounaros I, Cherevko S, Zeradjanin AR, Mayrhofer KJJ. Oxygen Electrochemistry as a Cornerstone for Sustainable Energy Conversion Angewandte 2014:102–21. <https://doi.org/10.1002/anie.201306588>.
- [41] Anantharaj S, Noda S. Amorphous Catalysts and Electrochemical Water Splitting : An Untold Story of Harmony 2019;1905779:1–24. <https://doi.org/10.1002/sml.201905779>.
- [42] Quan S, Wen DX. Hierarchical hollow heterostructures for photocatalytic CO₂ reduction and water splitting 2020;4. <https://doi.org/10.1002/smt.201900586>.
- [43] Corma A, Garcia H. Photocatalytic reduction of CO₂ for fuel production : Possibilities and challenges. J Catal 2013:2–9. <https://doi.org/10.1016/j.jcat.2013.06.008>.
- [44] Manuscript A. Chemical Science 2016. <https://doi.org/10.1039/C6SC00077K>.
- [45] Mechanochemistry : towards sustainable design of advanced nanomaterials for electrochemical energy storage and catalytic applications 2018. <https://doi.org/10.1021/acssuschemeng.8b01716>.
- [46] Datta A, Das K, Beyene BB, Garribba E, Gajewska MJ, Hung C. EPR interpretation and electrocatalytic H₂ evolution study of bis (3 , 5-di-methylpyrazol-1-yl) acetate

- anchored Cu (II) and Mn (II) complexes. *Mol Catal* 2017;439:81–90. <https://doi.org/10.1016/j.mcat.2017.06.024>.
- [47] Yang M, Zhou Y, Cao Y, Tong Z, Dong B, Chai Y. Advances and Challenges of Fe-MOFs Based Materials as Electrocatalysts for Water Splitting. *Appl Mater Today* 2020;20:100692. <https://doi.org/10.1016/j.apmt.2020.100692>.
- [48] Chen P, Ye J, Wang H, Ouyang L, Zhu M. water splitting. *J Alloys Compd* 2021;883:160833. <https://doi.org/10.1016/j.jallcom.2021.160833>.
- [49] Peng X, Yan Y, Jin X, Huang C, Jin W, Gao B, et al. *Journal of Nano Energy* 2020;105234. <https://doi.org/10.1016/j.nanoen.2020.105234>.
- [50] Zhang L, Xiao J, Wang H, Shao M. Carbon-based Electrocatalysts for Hydrogen and Oxygen Evolution Reactions Department of Chemical and Biological Engineering , Hong Kong University of Science College of Electrical and Optoelectronic Engineering , Changzhou Institute of College of Chemistry and Chemical Engineering , Central South University , Changsha 2017. <https://doi.org/10.1021/acscatal.7b02718>.
- [51] Wang C, Wang A, Zhao S, Li X, Sun D, Jiang J, et al. *Materials Chemistry A* 2018. <https://doi.org/10.1039/C8TA02839G>.
- [52] Hu C, Dai L. Multifunctional Carbon-Based Metal-Free Electrocatalysts for Simultaneous Oxygen Reduction , Oxygen Evolution , and Hydrogen Evolution 2017:1–9. <https://doi.org/10.1002/adma.201604942>.
- [53] Zhang W, Lin N, Liu D, Xu J, Sha J, Yin J, et al. Direct carbonization of rice husk to prepare porous carbon for supercapacitor applications. *Energy* 2017;128:618–25. <https://doi.org/10.1016/j.energy.2017.04.065>.
- [54] Online VA, Gujjarahalli CT. *RSC Advances* 2014. <https://doi.org/10.1039/C4RA05135A>.
- [55] Manuscript A. *ChemComm* 2017. <https://doi.org/10.1039/C6CC09187C>.
- [56] Salame P, Pawade V, Bhanvase BA. Characterization Tools and Techniques for Nanomaterials. 2018. <https://doi.org/10.1016/B978-0-12-813731-4.00003-5>.
- [57] Kaliva M, Vamvakaki M. Chapter 17 - Nanomaterials characterization. Elsevier Inc.; 2020. <https://doi.org/10.1016/B978-0-12-816806-6.00017-0>.

- [58] Titus D, Samuel EJJ, Roopan SM. Chapter 12 - Nanoparticle characterization techniques. Elsevier Inc.; 2019. <https://doi.org/10.1016/B978-0-08-102579-6.00012-5>.
- [59] Shanks RA. Characterization of Nanostructured Materials. Elsevier Inc.; 2014. <https://doi.org/10.1016/B978-1-4557-3159-6.00002-X>.
- [60] Buckley K, Matousek P. Journal of Pharmaceutical and Biomedical Analysis Recent advances in the application of transmission Raman spectroscopy to pharmaceutical analysis. *J Pharm Biomed Anal* 2011;55:645–52. <https://doi.org/10.1016/j.jpba.2010.10.029>.
- [61] Ferrari AC, Robertson J, Trans P, Lond RS. Raman spectroscopy of amorphous , nanostructured , diamond – like carbon , and nanodiamond 2004:2477–512. <https://doi.org/10.1098/rsta.2004.1452>.
- [62] Bumrah GS, Sharma RM. Raman spectroscopy – Basic principle , instrumentation and selected applications for the characterization of drugs of abuse. *Egypt J Forensic Sci* 2016;6:209–15. <https://doi.org/10.1016/j.ejfs.2015.06.001>.
- [63] ScienceDirect_citations_1696237780899 n.d.
- [64] Hans-Jürgen Butt, Karlheinz Graf MK. Physics and Chemistry of Interfaces. John Wiley & Sons; n.d.
- [65] Vis UVÀ, Yurdakal S, Garlisi C, Levent O, Bellardita M, Palmisano G. Techniques : Adsorption Isotherms and. vol. 4. 2019. <https://doi.org/10.1016/B978-0-444-64015-4.00004-3>.
- [66] Khan R, Taqi M, Mahmood M, Sarfraz B, Raza S, Bilal M, et al. 3D hierarchical heterostructured LSTN @ NiMn-layered double hydroxide as a bifunctional water splitting electrocatalyst for hydrogen production. *Fuel* 2021;285:119174. <https://doi.org/10.1016/j.fuel.2020.119174>.
- [67] Prahas D, Kartika Y, Indraswati N, Ismadji S. Activated carbon from jackfruit peel waste by H₃PO₄ chemical activation : Pore structure and surface chemistry characterization 2008;140:32–42. <https://doi.org/10.1016/j.cej.2007.08.032>.
- [68] U nderstanding chemical reactions between carbons and NaOH and KOH An insight into the chemical activation mechanism 2003;41:267–75.

- [69] Manuscript A. www.rsc.org/njc n.d.
- [70] Bhattacharya S, Dinda D, Saha SK. Role of trap states on storage capacity in a graphene / MoO₃ 2D electrode material 2015. <https://doi.org/10.1088/0022-3727/48/14/145303>.
- [71] Yurdakal S. (Photo) catalyst Characterization Techniques. vol. 331307484. 2019. <https://doi.org/10.1016/B978-0-444-64015-4.00004-3>.
- [72] Stoller MD, Park S, Zhu Y, An J, Ruoff RS. Graphene-Based Ultracapacitors 2008:6–10.
- [73] Simon P, Gogotsi Y. Materials for electrochemical capacitors n.d.:845–54.
- [74] Hoang VC, Dinh KN, Gomes VG. Hybrid Ni/NiO composite with N-doped activated carbon from waste cauliflower leaves: A sustainable bifunctional electrocatalyst for efficient water splitting. Carbon N Y 2019. <https://doi.org/10.1016/j.carbon.2019.09.080>.
- [75] Cho S, Jeon H, Son Y, Lee S, Kim T. ScienceDirect Water splitting over an ultrasonically synthesized NiFe / MoO₃ @ CFP electrocatalyst. Int J Hydrogen Energy 2023;48:26032–45. <https://doi.org/10.1016/j.ijhydene.2023.03.236>.
- [76] Song Y, Wang P, Baek J. Controlled synthesis of highly active bifunctional electrocatalysts for overall water splitting using coal-based activated carbons 2023;11. <https://doi.org/10.1039/d2ta06595a>.
- [77] Ashraf I, Ahmad S, Rizwan S, Iqbal M. Fabrication of Ti₃C₂ @ MoO₃ nanocomposite as an electrode material for highly efficient and durable water splitting system. Fuel 2021;299:120928. <https://doi.org/10.1016/j.fuel.2021.120928>.
- [78] Davodi F, Tavakkoli M, Lahtinen J, Kallio T. Straightforward synthesis of nitrogen-doped carbon nanotubes as highly active bifunctional electrocatalysts for full water splitting. J Catal 2017;353:19–27. <https://doi.org/10.1016/j.jcat.2017.07.001>.